Hindawi
Adsorption Science & Technology
Volume 2022, Article ID 5935712, 18 pages
https://doi.org/10.1155/2022/5935712

Research Article

Ecofriendly Biosorbents Produced from Cassava Solid Wastes: Sustainable Technology for the Removal of Cd^{2+}, Pb^{2+}, and Cr^{total}

Daniel Schwantes,[1] **Affonso Celso Gonçalves Junior**,[2] **Henrique Alipio Perina**,[3] **César Ricardo Teixeira Tarley**,[4] **Douglas Cardoso Dragunski**,[5] **Elio Conradi Junior**,[2] **and Juliano Zimmermann**[2]

[1]*Pontifícia Universidad Católica de Chile, Avenida Vicuña Mackenna no. 4860, Santiago, Macul, Región Metropolitana, Chile*
[2]*Universidade Estadual do Oeste do Paraná, Rua Universitária, No. 1619, Universitário, Cascavel, State of Paraná, Brazil*
[3]*Pontifícia Universidade Católica do Paraná, Avenida União, No. 500, Toledo, State of Paraná, Brazil*
[4]*Universidade Estadual de Londrina, Rod. Celso Garcia Cid, State of Paraná, 445 Km 380, Campus Universitário, Londrina, State of Paraná, Brazil*
[5]*Universidade Estadual do Oeste do Paraná, Rua da Faculdade, No. 645, Jardim La Salle, Toledo, State of Paraná, Brazil*

Correspondence should be addressed to Daniel Schwantes; daniel_schwantes@hotmail.com

Received 8 October 2021; Revised 5 January 2022; Accepted 9 February 2022; Published 9 March 2022

Academic Editor: Muhammad Raziq Rahimi Kooh

This research is aimed at investigating the possible use of cassava agroindustry solid wastes in manufacturing adsorbents and their use in removing heavy metals Cd^{2+}, Pb^{2+}, and Cr^{total} from water. Thus, a pilot study was conducted in two main steps: (1) obtaining and characterizing the adsorbents and (2) laboratory studies focused on the evaluation of critical physicochemical parameters on adsorption, such as pH of the solution containing heavy metals, the effect of adsorbent dose, besides kinetics and equilibrium adsorption and desorption studies. Three adsorbents were studied, cassava barks, bagasse, and their mixture. SEM, FTIR, pH_{PZC}, acid digestion, and chemical composition analysis were employed for adsorbent characterization. The pH of the contaminated solution was evaluated within 4.0 to 7.0, while the adsorbent doses varied from 5.0 to 24.0 g L^{-1}. The adsorption kinetics was evaluated within 5 to 180 minutes and interpreted using pseudofirst- and second-order models. Finally, equilibrium and desorption studies were performed by evaluating adsorbent performance within 5 to 200 mg L^{-1} of heavy metals, using several nonlinear models for results interpretation. SEM analysis reveals a heterogeneous structure full of cavities. FTIR before and after adsorption reveals gaps related to missing functional groups, suggesting a significant role of alkenes, carboxylic acid, alcohol, anhydride, and ether. pH_{PZC} is found at pH 6.02, 6.04, and 6.26 for adsorbents derived from barks, bagasse, and their mixture. In low concentrations of metals, the higher adsorption capacities were found at pH 7.0 (94.9%) using 16 g L^{-1} of adsorbent, with the most cost-benefit dose found using 8.0 g L^{-1}. The removal of metals reaches equilibrium within 5-10 minutes of contact time with pseudosecond-order best adjustments to the observed phenomena. The adsorption of metals by a cassava adsorbent is better adjusted to the Freundlich model, with significant and critical information provided by Sips, Redlich-Peterson, Temkin, Liu, and Khan models. Adsorption/desorption studies indicate that cassava adsorbent performs, on average, -10% of the adsorption of metals compared to activated carbon. Nevertheless, factors such as low cost and availability favor the use of such natural materials.

1. Introduction

In the last decade, the increasing industrialization and urbanization have raised the number of pollutants disposed of in the environment, especially water bodies [1]. In this sense, among the many contaminants that affect aquatic environments and human health, the pollution from organic or inorganic compounds, such as toxic metals and metalloids (Cd, Pb, Cr, As,

Hg, among others) and pesticides (organophosphates, carbamates, triazines, organochlorines, among others.) need to be treated as a serious issue by governs and institutions. Moreover, access to fresh water and sanitation still is a global concern. For example, WHO [2] reports that 785 million people lack even a basic drinking water service, including 144 million people who are dependent on surface water; globally, at least 2 billion people use a drinking water source contaminated with feces, that is not to mention water pollution by chemicals, such as toxic heavy metals.

Developing and undeveloped countries already struggle with the standard procedures and cannot afford more advanced technologies to treat emergent pollutants such as pesticides and metals [3]. Among the advanced treatments that are usually employed for the removal of toxic metals, we can highlight chemical and physical precipitation, ionic exchange, Fenton and photo-Fenton processes, oxidation processes, filtration by membranes, osmosis processes, advanced oxidation processes, and adsorption with activated carbons; this last example is considered a gold standard for the removal of many organic and inorganic pollutants from waters and wastewaters [4], especially when those are in low (or trace) concentrations but not low enough to ensure the safety of the disposal of the wastewater or the use of water [5–7]. That is the case with heavy toxic metals [8].

The current legislation for drinking water by Environmental Protection Agency [9], World Health Organization [4], and *Ministerio de Salud de Chile* [10], respectively, state the maximum contaminant level for the studied metals: Cd^{2+} ($0.005\,mg\,L^{-1}$, $0.003\,mg\,L^{-1}$, and $0.01\,mg\,L^{-1}$), Pb^{2+} ($0.015\,mg\,L^{-1}$, $0.01\,mg\,L^{-1}$, and $0.05\,mg\,L^{-1}$), and Cr^{total} ($0.01\,mg\,L^{-1}$, $0.05\,mg\,L^{-1}$, and $0.05\,mg\,L^{-1}$). Thus, the limits are low because such substances can promote damage to living organisms even at trace levels. Further information regarding toxicity and environmental issues caused by heavy metal exposure (with special attention to Cd, Pb, and Cr) are shown in the Supplementary Materials.

Another problem that causes significant concern in the agroindustry business is the correct biomass solid waste destination, e.g., solid byproducts from the cassava industry. These agroindustries tend to generate significant amounts of organic wastes, which can or cannot be correctly destined [3, 11–13], usually disposed of either by burning, dumping, or unplanned landfilling [14, 15].

In cassava agroindustry, solid wastes are generated in the processing of cassava roots, mainly used to manufacture animal feed and biofertilizers. Schwantes et al. [13] estimate that cassava peel makes up approximately 3 to 5% of the total mass of roots and about 1 million tons of cassava peels are produced annually in Brazil, 11 million tons worldwide. This estimate does not consider the produced bagasse, representing more than 80% of the cassava industry's solid wastes.

The last reports evidence the possibility of using cassava as adsorbent for the removal of Cd^{2+}, Pb^{2+}, and Cr^{total} from waters [16], or as biomass modified with H_2O_2, H_2SO_4, or NaOH 0.1 M [13], or for the removal of Cu^{2+} [17], Cu^{2+}, and Zn^{2+} [18]. Rajeshwarisivaraj et al. [19] report the use of cassava wastes impregnated with H_3PO_4 in activated carbon development to remove dyes and metal ions. Thompson et al. [20] reported using activated biomass from cassava wastes to remove Pb^{2+} from water. Although the above reports are interesting, Schwantes et al. [18], Schwantes et al. [13], and Schwantes et al. [16] present only preliminary studies, with many gaps regarding the adsorption process and its evaluation. Also, the above authors do not elucidate the adsorption mechanism that rules metals' removal. Jorgetto et al. [17] only used the minced cassava root as an adsorbent raw material, not focusing on the cassava bagasse, which corresponds to more than 90% of the wastes of cassava agroindustry. Moreover, the above authors only test the adsorbent for Cu^{2+} adsorption without the necessary deep required for adsorption studies (kinetics, equilibrium, and thermodynamic studies). Rajeshwarisivaraj et al. [19] tested cassava wastes as adsorbents for the removal of dyes (Rhodamine-B, direct brown, procion orange, acid violet, malachite green, and methylene blue) and metals (Cr^{6+}, Hg^{2+}, and Fe^{2+}) without evaluating the influence of essential parameters, such as pH, adsorbent doses, contact time, equilibrium, and thermodynamic studies. Thompson et al. [20] developed activated carbon from solid cassava wastes, resulting in a material gifted with $119.6\,m^2$ and good adsorption capacity, nevertheless, with inferior results comparing other adsorbents and activated carbons derived from adsorbent materials. Therefore, there is still a lack of studies regarding cassava solid wastes for adsorption purposes. Thus, such raw materials are still undervalued and unexploited.

In this scenario, this research attempts to propose solutions for two problems (environmental and public health) at the same time: first, to develop natural ecofriendly adsorbents from cassava agroindustry solid wastes for the remediation of water containing toxic metals (Cd^{2+}, Pb^{2+}, and Cr^{total}), providing an economical and novel solution for water and wastewater treatment, especially attractive for undeveloped/developing countries; and the second part of the double solution, to provide a correct and possible destination for the risen tons of agro-industrial cassava wastes, which already are, in some cases, environmental problems in developing countries located in South America, Africa, and equatorial parts of Asia.

Thus, until this date, the potential of solid cassava wastes has not been fully accessed in developing ecofriendly and efficient adsorbents, especially for removing heavy metals such Cd^{2+}, Pb^{2+}, and Cr^{total}. As a consequence, this research aimed at (i) developing natural adsorbents from cassava agroindustries and studying its morphology and other essential characteristics; (ii) evaluating these natural materials regarding their adsorption capacity and performance; (iii) studying the adsorption mechanism of Cd^{2+}, Pb^{2+}, and Cr^{total}, evaluating the interactions between the pH of the metal solutions versus dose of adsorbents, as well as studies of kinetics and equilibrium; and (iv) evaluating the possibility of the cassava adsorbents reuse in new cycles (desorption studies).

2. Material and Methods

2.1. Obtaining, Development, and Characterization of the Cassava Natural Adsorbents. In agroindustry, the cassava

wastes were obtained from Toledo, Paraná State (Brazil). During the cassava root preparation for further processing, the first solid waste is obtained (cassava barks) by the washing and mechanical peeling of the roots, constituted mainly of lignin and cellulose. After removing starch and other essential components, the second solid waste (bagasse) was obtained at the end of the industrial process. The bagasse is constituted mainly by lignin, cellulose, and residues of nonextracted starch.

It is essential to mention that the agroindustrial cassava sector destines these wastes for animal feeding by mixing a small proportion of barks with bagasse selling them to cattle and cow farmers as a low-cost feed. Therefore, these wastes were sampled and sent to the laboratory, washed with water, dried, milled, and sieved, with particle size standardized between 14 to 60 mesh, as already well reported by previous studies [18]. This procedure generated the three adsorbents of cassava: CASS-BK (adsorbent of cassava barks), CASS-BA (adsorbent of cassava bagasse), and CASS-BB (the mix of barks and bagasse of cassava). These three were characterized by studying their surface by pH_{PZC} analysis, micrographs by SEM, surface functional groups by FTIR, and their chemical composition.

The pH corresponding to the point of zero charge (pH_{PZC}) is defined as the pH at which the surface of the solid has a neutral charge. The methodology used in this work for its determination is called the "11 point experiment" [3]. The procedure consisted of mixing 25 mg of the adsorbent in 50 mL of aqueous solutions of KCl 0.5 and 0.05 M under 11 different conditions of initial pH, varying from 2.0 to 13.0 by adjustment with HCl and NaOH (0.1 mol L^{-1}), and measuring the pH after 24 h of equilibrium. The results are expressed through the graph of final pH versus initial pH, with the pH_{PZC} corresponding to the range in which the final pH remains constant (regardless of the initial pH), i.e., the surface behaves like a buffer. The surface micrographs were obtained using scanning electron microscopy (SEM - JEO JSM 6360-LV, Thermo®, U.S.A), equipped with dispersive energy microscopy. The surface functional groups were characterized using an FTIR-8300 Fourier transform spectrometer operating in transmission mode (4000–400 cm^{-1}), using the standard KBr pellet method (Shimadzu®, Japan). The chemical composition of metals was analyzed by acid digestion of the cassava adsorbents [70], followed by FAAS determination. Thus, 0.5 mg of each adsorbent was weighted in test tubes with 5 mL of HNO_3+HClO mixture (2 : 1 *v*/*v*), maintained at 160°C for two hours and then at 260°C for another 1.5 h. After that, samples were transferred to 50 mL volumetric flasks. The concentration of K (wavelength of 766.5 nm), Ca (422.7 nm), Mg (285.2 nm), Fe (248.3 nm), Cu (324.8 nm), Zn (213.9 nm), Cd (228.8 nm), Pb (217.0 nm), and Cr (357.9 nm) was determined by Flame Atomic Absorption Spectrometry (FAAS, GBC 932 AA) [21].

2.2. Preparation of the Metallic Solutions. All single-element solutions of Cd, Pb, and Cr were prepared by using salts of cadmium ($Cd(NO_3)_2$ $4H_2O$ PA ≥ 99.0% Sigma-Aldrich), lead ($Pb(NO_3)_2$PA ≥ 99%, Sigma-Aldrich), and chromium ($Cr(NO_3)_3$ $9H_2O$ PA ≥ 99%, Sigma-Aldrich).

2.3. Adsorption Studies (Cd^{2+}, Pb^{2+}, and Cr^{total})

2.3.1. pH and Adsorbent Dose Studies. The effect of the pH of the single-element solutions of Cd^{2+}, Pb^{2+}, and Cr^{total} and its interaction with different cassava adsorbent doses was evaluated by testing three (3) pH conditions (4.0, 5.0, and 6.0, adjusted with NaOH and HCl 0.1 M) and six (6) adsorbent doses (4, 8, 12, 16, 20, and 24 g L^{-1}). Thus, in Erlenmeyer's of 125 mL, 200, 400, 600, 800, 1000, and 1200 mg of CASS-BK, CASS-BA, and CASS-BB were set in contact with 50 mL of the single-element solutions of Cd^{2+}, Pb^{2+}, and Cr^{total} (10 mg L^{-1}). The experimental condition of this preliminary study was 200 rpm at 25°C. At the end of 1.5 h of stirring, samples were taken, and the remaining metal concentration was determined by FAAS.

Using Statistica® 7.0, a response surface analysis (RSA) was conducted to interpret these preliminary results. Therefore, a weighted linear regression was used to study the possible interactions between the adsorbent doses and the solution pH. In addition, the Fisher test was conducted to determine the statistical significance of the variables above on the removal % of heavy metals. Finally, the Tukey test evaluated the removal percentage means at 5% of probability to create a ranking between the adsorbents and the evaluated metals. The studied pH range is explained by the Theoretical speciation of Cd^{2+}, Pb^{2+}, and Cr^{total} (Puigdomenech, 2018), presented in Figure S2 [22].

2.3.2. Kinetics Studies. In order to evaluate the effect of the contact time between the cassava adsorbents and the Cd^{2+}, Pb^{2+} and Cr^{total} single-element solutions, the adsorbent dose of 8.0 g L^{-1} (previous best condition) was tested in the following contact time ranges: 5, 10, 20, 40, 60, 80, 100, 120, 140, and 160 min.

Thus, in Erlenmeyer of 125 mL, 400 mg of CASS-BK, CASS-BA, and CASS-BB was set in contact with 50 mL of single-element solutions of Cd^{2+}, Pb^{2+}, and Cr^{total} solutions (10 mg L^{-1}), and samples were taken at each period (5 to 160 min), centrifuged at 2000 rpm for liquid-solid separation, and the remaining metal concentration was determined by FAAS.

To elucidate the kinetics of adsorption for Cd^{2+}, Pb^{2+}, and Cr^{total} into the CASS-BK, CASS-BA, and CASS-BB surfaces, the obtained data were studied by the models of pseudofirst-order (PFO) [23] and pseudosecond-order (PSO) [24] models, as exhibited in Table S1 (supplementary material).

2.3.3. Equilibrium Studies and Side-by-Side Comparison (Activated Carbon). In order to construct isotherms for CASS-BK, CASS-BA, and CASS-BB for the adsorption of metals, in Erlenmeyer of 125 mL, the dose of 8.0 g L^{-1} (400 mg) of cassava adsorbents was set in contact with 50 mL in increasing concentrations of Cd^{2+}, Pb^{2+}, and Cr^{total} single-element solutions (5, 20, 40, 60, 80, 100, 120, 140, 160, and 200 mg L^{-1}). The following experimental conditions were set at pH 5.5, 60 min of stirring, 200 rpm, and 25°C. The content (adsorbent solution) was centrifuged at 2000 rpm for liquid-solid separation and sampled to determine the residual metal concentration by FAAS.

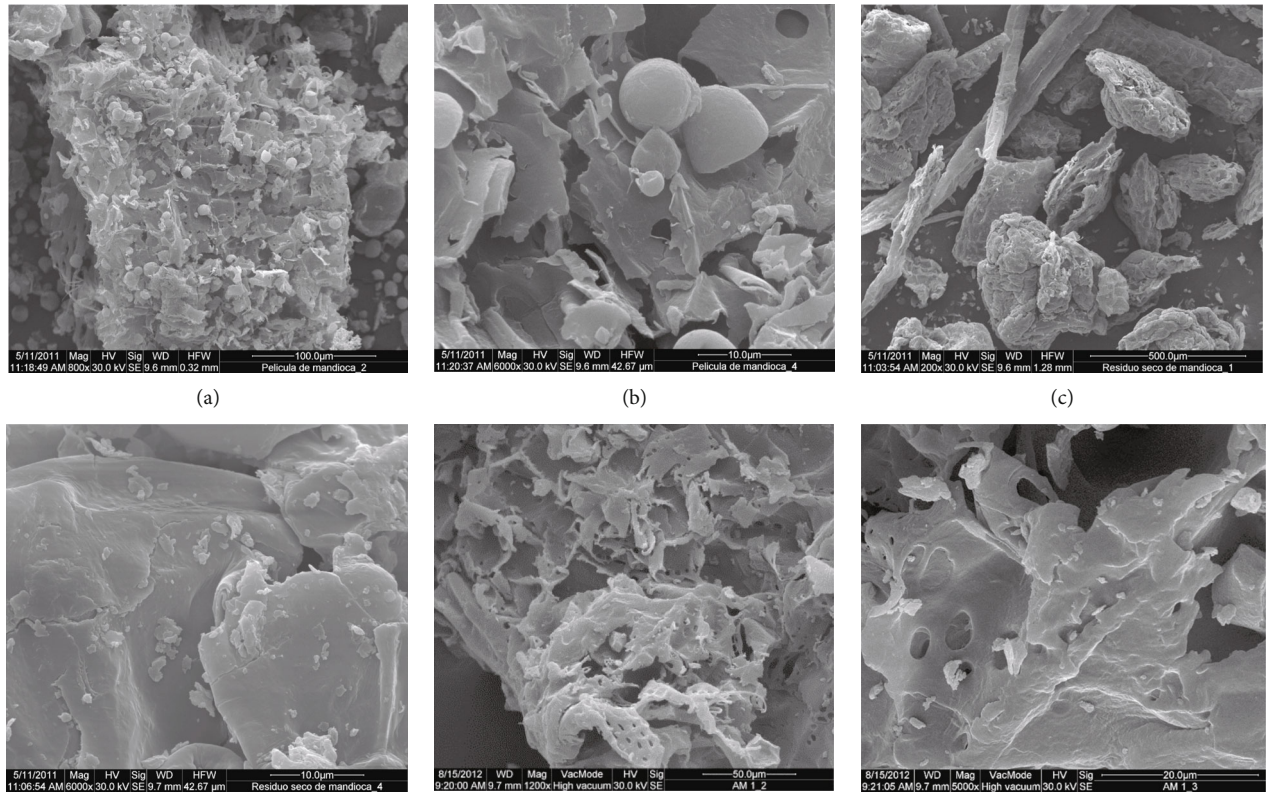

Figure 1: SEM of CASS-BK ((a, b) 800 and 6000x), CASS-BA ((c, d) 200 and 6000x), and CASS-BB ((e, f) 1200 and 5000x).

It is also essential to highlight that for the isotherm construction and evaluation, a side-by-side comparison was performed with a gold standard (commercial activated carbon Synth) in the same physical-chemical conditions CASS-BK, CASS-BA, and CASS-BB.

For the interpretation of the obtained data, the nonlinear models of Langmuir [25], Freundlich [26], Sips [27], Temkin and Pyzhev [28], Redlich-Peterson [29], Toth [30], Liu et al. [31], Khan et al. [32], and Khan et al. [33] were employed. These and other equations used in this research are exhibited in Table S1 (supplementary material).

2.3.4. Desorption studies. The possibility of reusing CASS-BK, CASS-BA, and CASS-BB was evaluated through an acid elution using HCl 0.1 mol L^{-1}. For that, after the isotherm's construction (after one adsorption cycle in different metal concentrations), the cassava adsorbents were dried at 60 ± 2°C for 24 h, and their mass was set into contact with 50 mL of HCl 0.1 mol L^{-1}. Then, after 60 min of 200 rpm stirring, samples were taken and centrifuged at 2000 rpm to separate the adsorbent acid solution, and FAAS determined the desorbed concentration of metal (Cd^{2+}, Pb^{2+}, and Cr^{total}). The estimative of the desorption rate (D) is exhibited in Table S1.

2.3.5. The Effect of Temperature on the Adsorption of Cd^{2+}, Pb^{2+}, and Cr^{total} by Cassava Adsorbents. To evaluate the effect of temperature on the adsorption of heavy metals, 400 mg of each adsorbent was weighed in 125 mL Erlenmeyer flasks and set in contact with 50 mL of Cd^{2+} (50 mg L^{-1}), Pb^{2+} (100 mg L^{-1}), or Cr^{total} (50 mg L^{-1}) solutions at pH 5.5. These flasks were stirred for 60 min at 25, 35, 45, 55, and 65°C. After that period, samples were taken and centrifuged at 2000 rpm to separate the adsorbent from the solution, and FAAS determined the remaining concentration of each metal. Thermodynamic parameters ΔG°, ΔH°, and ΔS°, were estimated according to Table S1.

2.4. Data Analysis. Maple 13®, Statistica 7®, Sisvar 5.6 [34], and Origin 2018® were employed to evaluate the aforementioned nonlinear models, besides the construction of the graphics. All values from adsorption studies were obtained in triplicate. Also, the studied models were subjected to reduced chi^2, R-square (COD), and adjusted R^2 analysis.

3. Results and Discussion

3.1. Characterization of the Cassava Natural Adsorbents. The CASS-BK, CASS-BA, and CASS-BB surfaces revealed by SEM (Figure 1) reveal adsorbents endowed with fibrous and spongy aspects, with irregular and heterogeneous structures. In addition, it is possible to observe some cavities, which could indicate the structure's porosity, which is suggested as a promising adsorbent characteristic by Conradi Jr. et al. [3].

Figure 2 and Table S2 show infrared spectroscopy absorption by frequency regions from before and after the adsorption of Cd^{2+}, Pb^{2+}, and Cr^{total}. The abovementioned

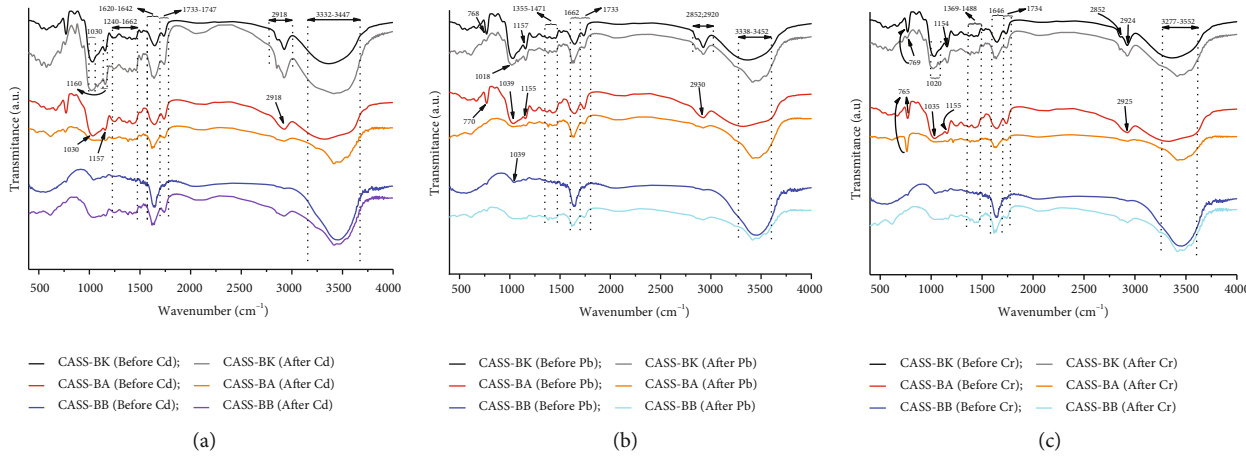

Figure 2: FTIR obtained for the cassava natural adsorbents CASS-BK (a), CASS-BA (b), and CASS-BB (c) before and after the adsorption of Cd^{2+}, Pb^{2+}, and Cr^{total}. Additional information is provided in Table S2.

Table 1: Composition of K, Ca, and Mg (g kg^{-1}) and Cu, Fe, Mn, Zn, Cd, Pb, and Cr (mg kg^{-1}) of the cassava adsorbents.

Adsorbent	K	Ca	Mg	Cu	Fe	Mn	Zn	Cd	Pb	Cr
	g kg^{-1}			mg kg^{-1}						
CASS-BK	24.10 ± 1.36	35.03 ± 1.36	6.83 ± 0.38	14.33 ± 0.57	35.67 ± 6.43	123.33 ± 1.52	32.00 ± 1.00	<LQ	11.00 ± 0.08	<LQ
CASS-BA	5.77 ± 0.49	23.23 ± 0.49	4.58 ± 0.10	5.67 ± 0.57	24.50 ± 4.50	27.67 ± 0.57	18.67 ± 0.57	<LQ	14.67 ± 0.57	<LQ
CASS-BB	7.77 ± 0.68	22.58 ± 0.69	5.12 ± 0.30	6.00 ± 1.00	26.00 ± 3.00	34.00 ± 13.89	17.00 ± 1.00	<LQ	3.33 ± 1.15	<LQ

Notes: LQ: limits of quantification: K = 0.01, Ca = 0.005, Mg = 0.005, Cu = 0.005, Fe = 0.01, Mn = 0.01, Zn = 0.005, Cd = 0.005, Pb = 0.01, and Cr = 0.01 (mg kg^{-1}).

results highlight the missing peaks at 760 cm^{-1} for CASS-BK adsorption of Cd^{2+} and Pb^{2+}, suggesting C=C medium to strong bending of alkenes [35].

Comparing the results from before and after adsorption, there are many gaps for CASS-BA, such as 769, 1030, 1157, 1240-1662, and 2930 cm^{-1} for Cd^{2+} adsorption, suggesting a significant role by C=C from alkenes; CO-O-CO from anhydride; C-O from alcohol and aliphatic ether; C-H and O-H from alkanes, carboxylic acid, and alcohol; and C-H stretching from alkanes [36]. For Pb^{2+} adsorption by CASS-BA, gaps were found at 770, 1039, and 1155 cm^{-1}, indicating C=C bending from alkenes, CO-O-CO stretching from anhydride, C-O from alcohol and ether, and C-H stretching from alkanes [37]. For Cr^{total} adsorption by CASS-BA, gaps were found at 1035 and 1155 cm^{-1}, suggesting CO-O-CO stretching from anhydride and C-O stretching from secondary alcohol and aliphatic ether and C-H stretching from alkanes [61]; [37].

CASS-BB gaps are found for Cd^{2+} adsorption at 1733-1744 cm^{-1} strong C=O stretching from conjugated anhydride, esters, and aldehyde and Pb^{2+} adsorption 1039 cm^{-1}, from medium C-H stretching from alkanes [38].

The pH_{PZC} values of the cassava natural adsorbents were 6.02 ± 0.06 to CASS-BK, 6.04 ± 0.27 to CASS-BA, and 6.26 ± 0.16 to BASS-BB (Figure S1). Thus, for environment pH higher than the pH_{PZC}'s (6.02, 6.04, or 6.26), negative charges should predominate in the cassava adsorbent materials surface, favoring cation adsorption, such as heavy metal ions. Moreover, the CONAMA [39] guidance for natural water bodies states that natural waters tend to be found with pH values around 9 to 10, favoring heavy metals adsorption if these are in the aqueous medium.

Gonçalves Junior et al. [40], studying canola-based adsorbents, found values ranging from 5.95 to 6.04. Gonçalves Junior et al. [41], studying *Euterpe Oleracea*-based adsorbent, found 5.09 as pH_{PZC}. Schwantes et al. [42, 43] found 5.67 for a crambe-based adsorbent (*Crambe abyssinica* Hochst). Schwantes et al. [12] found 4.28 for the grape steam adsorbent. All the above authors conducted adsorption studies with pH values within the range 4.0 to 7.0, mainly due to the surface functional groups from lignin and cellulose structures that all the above adsorbents have in common and because heavy metals such as Cd^{2+}, Pb^{2+}, and Cr^{total} tend to precipitate in higher pH values.

When the $pH_{PZC} > pH_{environment}$, the adsorbent surface is predominantly protonated (electropositive), favoring anion adsorption. On the other hand, when $pH_{PZC} < pH_{environment}$ the adsorbent surface is negatively charged, i.e., favoring cation adsorption [12].

The chemical composition of the cassava adsorbent (Table 1) is evidence around 22.5 to 35 g kg^{-1} of Ca, 5.7 to 24 g kg^{-1} of K, and 4.5 to 6.8 g kg^{-1} of Mg. CASS-BK presents the higher concentration of Mn (123 mg kg^{-1}), while CASS-BA and CASS-BB present 27.6 and 34.0 mg kg^{-1}, respectively. Fe concentrations were found around 35.6 and 4.5 mg kg^{-1}, while Zn was found around 17.0 and 32.0 mg kg^{-1}.

Minor Pb levels were found in the cassava adsorbent composition, about 3.3 to 14.6 mg kg^{-1}. The lead is probably

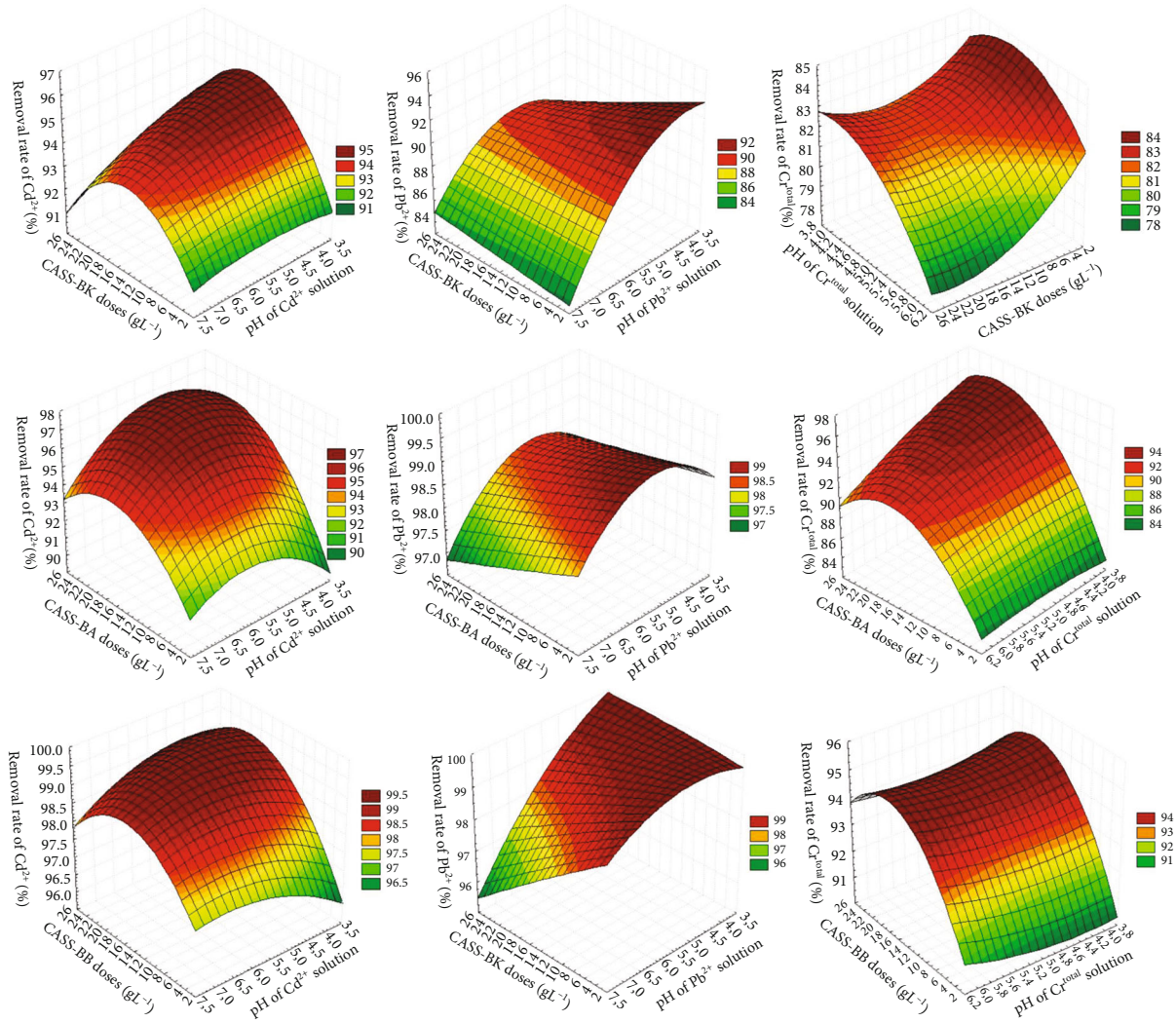

FIGURE 3: The influence of pH and the adsorbent doses on removing Cd^{2+}, Pb^{2+}, and Cr^{total} by CASS-BK, CASS-BA, and CASS-BB. Experimental conditions: adsorbent doses tested from 4.0 to 24 g L^{-1}, pH evaluated from 4.0 to 7.0, stirring at 160 rpm, at 298 K for 1.5 h.

from (1) industrial contamination during the cassava roots processing, or (2) it was absorbed from the soil by the cassava plants and accumulated in the roots. Bassegio et al. [1] report that Pb is not translocated to upper vegetal organs, primarily accumulated in roots. This element was only detected because the adsorbent was submitted to strong acid digestion, which released the Pb bonded to the lignocellulosic structure of the adsorbent. Pb release in water samples was not observed.

3.2. Adsorption Studies (Cd^{2+}, Pb^{2+}, and Cr^{total})

3.2.1. pH and Adsorbent Dose Studies. Table S3 shows the regression coefficients from Figure 3, while Table S4 shows the analysis of variance (ANOVA). Figure 4 illustrates the regression analysis for adsorbent doses. Finally, Table S3 shows the ideal pH and adsorbent dose conditions for the higher removal of heavy metals.

The variable "Adsorbent" is significant at 1% of probability for Cd^{2+}, Pb^{2+}, and Cr^{total} removal, which means that there are differences in the removal rate of metal regarding the adsorbent (CASS-BK, CASS-BA, and CASS-BB). Furthermore, the parameter "Doses" is significant at 1% of probability for Cd^{2+}, and 5% for Pb^{2+} removal, evidencing that the adsorbent doses influence heavy metal removal. Also, for Pb^{2+} removal, the variable "pH" of solution and the interaction between "Adsorbent" and "pH" presented statistical differences.

Tukey's range test (Table S5) evidence the higher removal percentages at pH 5.0 for Cd^{2+} and Pb^{2+}, while tested doses or pH values did not provoke statistical differences for Cr^{total}. Regarding the tested adsorbents, CASS-BB presented the higher removal of Cd^{2+} (98.8%). CASS-BA (98.6%) and CASS-BB (98.9%) had the highest Pb^{2+} removal percentages, while CASS-BB (93.7%) had the highest Cr^{total} removal percentage. The interaction between the evaluated factors "pH" and "dose" is provided in Table S7.

On the other hand, Tukey's test range for the interaction between "Adsorbent" and "pH" (Table S7, Figure 3 and Figure S3) evidenced that CASS-BA presented higher means for Cd^{2+} removal at pH 6.0 (95.88%). CASS-BK

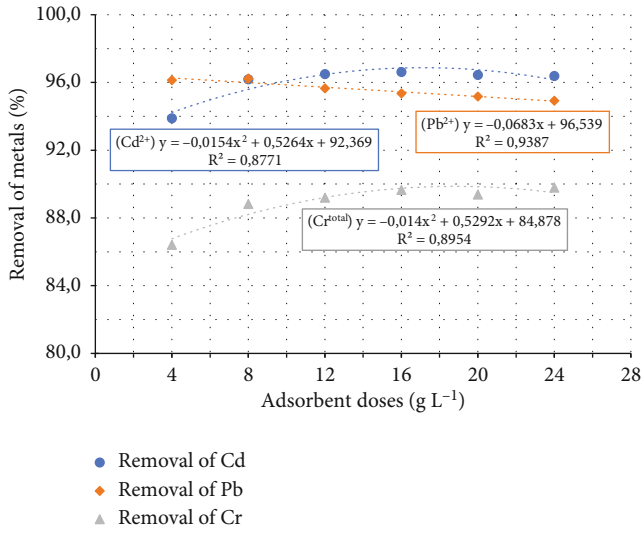

FIGURE 4: Regression analysis for the adsorbent doses (4.0 to 24.0 g L^{-1}) and its performance in removing Cd^{2+}, Pb^{2+}, and Cr^{total}. Note: additional information regarding this figure is provided in Table S6.

presented higher means for Pb^{2+} removal at pH 4.0 and 5.0 and CASS-BA (99.96%) and CASS-BB (92.53%) at pH 5.0. Furthermore, CASS-BB presented higher removal of Cr^{total} at pH 4.0.

Figure S3(a) shows a comparison between the removal percentage of the heavy metals (mean of Cd^{2+}, Pb^{2+}, and Cr^{total}) and the cassava-based adsorbents, where the following order is observed: CASS – BB (97.5%) > CASS – BA (95.5%) > CASS – BK (88.8%). Figure S3(b) shows the small variation observed for the averages of heavy metals removal in function to the pH evaluated range: pH 7.0 (94.9%) > pH 5.0 (94.3%) > pH 4.0 (93.9%) > pH 6.0 (92.9%) . Figure S3(c) highlights the small variation for the averages of heavy metals removal in function to the adsorbent doses: 16 g L^{-1} (94.3%) > 8.0 g L^{-1} (94.2%) = 12 g L^{-1} (94.2 %) > 20 g L^{-1} (94.1%) = 24 g L^{-1} (94.1%) > 4.0 g L^{-1} (92.7%).

Gonçalves Junior et al. [40] evaluated 16 canola-based adsorbents and reported the best adsorption rates using about 4.0 g L^{-1} to remove Pb^{+2}. The above authors did not find significant variations in the studied pH range (4.0 to 7.0) on Pb^{2+} removal. However, Gonçalves Junior et al. [41] found a statistical difference for adsorbent doses and pH of Cd^{+2} solution using *Euterpe Oleracea* endocarp-based adsorbent. The above authors report that 4.0 g L^{-1} produced the higher removing percentage of Cd^{2+}, Pb^{2+}, and Cr^{total} from water, and, in the case of Cd^{2+} adsorption systems, the pH ranges from 6.0 to 7.0 presented higher removal rates. Similarly, Schwantes et al. [42, 43] found no pH dependency (from 3.0 to 7.0) on adsorption of Zn by crambe-based adsorbents, being the adsorbent dose the primary influencer on Zn removal. In their studies, the higher Zn removal rates were found using 5.0 g L^{-1}. On the other hand, Schwantes et al. [12] found statistical differences only for the adsorbent doses, with higher removal of Cd^{2+} found using 5.0 g L^{-1} of grape steam-based adsorbent. These authors also claim that the evaluated pH range (3.0 to 7.0) did not influence Zn adsorption.

It is essential to state that heavy metal ions such as Cd, Pb, and Cr are only available for adsorption when dissolved in water solution, i.e., ions. Therefore, variations on the medium pH can cause the formation of complexes and favor their precipitation. For example, the theoretical diagram provided in Figure S2 illustrates the formation of different Cd, Pb, and Cr complexes in solution in pH > 7.0 [22]. Thus, as this research is aimed at optimizing the conditions for adsorption of heavy metals and comparing cassava adsorbents to activated carbon, we only evaluated pH conditions that could not cause the complexation and precipitation of such substances.

3.2.2. Kinetics Studies. Figure 5 shows that the adsorption of Cd^{2+}, Pb^{2+}, and Cr^{total} by the cassava-based adsorbents is a relatively fast process, with 90% of the removal achieved within 5 minutes of contact adsorbent metal in solution, with the physicochemical equilibrium reached between 5 and 10 min. This result is an essential and technological advantage when the industrial use of cassava adsorbents is considered for wastewater treatment.

The goodness of the fit obtained for PFO (Adj. R^2, R -square (COD), and reduced Chi^2] suggests this model's effectiveness in predicting the adsorption of heavy metals by the cassava-based adsorbents (Table 2). Nevertheless, there is a massive discrepancy by comparing the values of the amount of metal adsorbed estimated by the model (q_e calc.) and the experimentally obtained (q_e exp.).

Therefore, PFO does not predict the observed phenomena correctly. On the other hand, the goodness of the fit obtained for PSO (Adj. R^2, R-square (COD), and reduced Chi^2), and the excellent proximity between q_e calc and q_e exp strongly indicate that PSO efficiently predicts heavy metals' adsorption by cassava-based adsorbents, being the most suitable model. Consequently, the removal of Cd^{2+}, Pb^{2+}, and Cr^{total} appear to be ruled by chemical forces, such as ionic or covalent bond processes [24].

Silveira Neta et al. [44] report that PFO and PSO models assume that the difference between the adsorbed concentration at a given time and the equilibrium adsorbed concentration is the driving force of adsorption. Furthermore, the global adsorption rate is either proportional to the driving force in the PFO equation or is the square of the driving force for the PSO model.

The PSO velocity constant (k_2 expressed in g mg^{-1} min^{-1}) presented the following values for Cd^{2+} adsorption: $k_{2\,CASS-BB} = 8.47 > k_{2\,CASS-BA} = 2.54 > k_{2\,CASS-BK} = 2.50$, while for Pb^{2+} adsorption the following order is observed: $k_{2\,CASS-BB} = 3.82 > k_{2\,CASS-BA} = 2.35 > k_{2\,CASS-BK} = 1.88$; finally, for Cr^{total} adsorption, the following order is observed: $k_{2\,CASS-BB} = 11.45 > k_{2\,CASS-BK} = 4.30 > k_{2\,CASS-BA} = 2.47$. Regarding the estimated adsorbed amount (q_e calc., expressed in mg g^{-1}), for Cd^{2+} the following order is observed: q_e exp.$_{CASS-BB} = 1.24 > q_e$ exp.$_{CASS-BA} = 1.21 > q_e$ exp.$_{CASS-BK} = 1.20$; for Pb^{2+} adsorption: q_e exp.$_{CASS-BB} = 1.23 = q_e$ exp.$_{CASS-BA} = 1.23 > q_e$ exp.$_{CASS-BK} = 1.15$; and

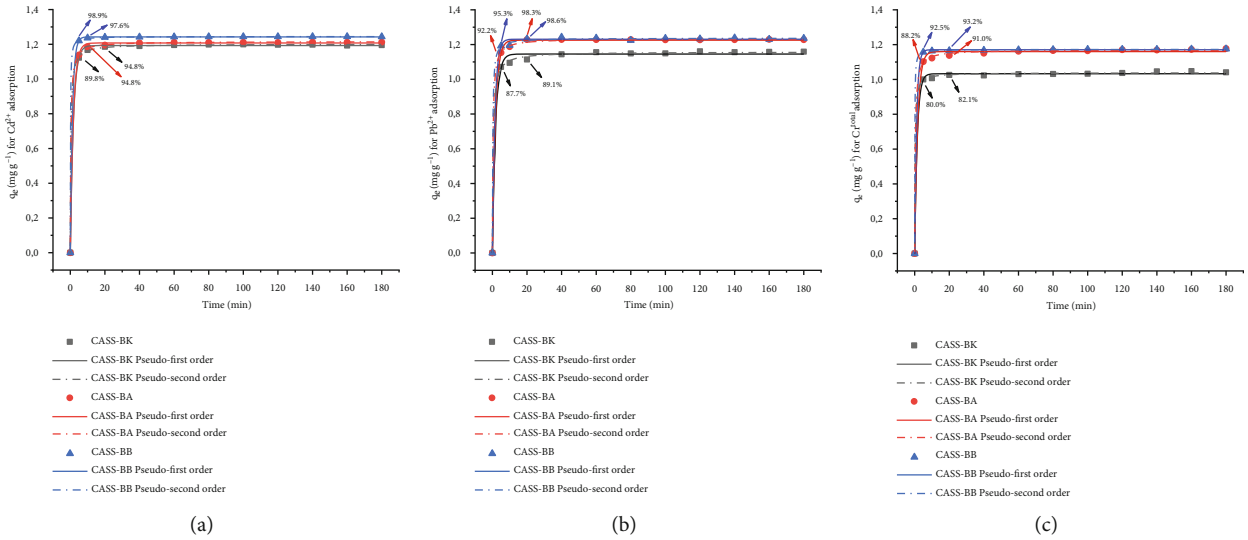

FIGURE 5: Kinetics of Cd^{2+} (a), Pb^{2+} (b), and Cr^{total} (c) adsorption by CASS-BK, CASS-BA, and CASS-BB. Experimental conditions: adsorbent dose of 8.0 g L^{-1}, pH of 5.5, stirring at 160 rpm, at 298 K, during 5, 10, 20, 40, 60, 80, 100, 120, 140, 160, and 180 min.

for Cr^{total} adsorption: q_e exp.$_{CASS-BB} = 1.17 = q_e$ exp.$_{CASS-BA} = 1.17 > q_e$ exp.$_{CASS-BK} = 1.04$. Considering the above, CASS-BB is the fastest cassava adsorbent for heavy metal adsorption, with also the highest values of adsorbed amount.

Wu et al. [45] developed hydrothermal activated carbon from cassava slag biochar. The authors found q_e of 24.10 mg g^{-1} for Rhodamine-B removal, with K_2 (g mg^{-1} min^{-1}) = 0.019, i.e., much smaller than the lowest found in this study for Cd^{2+} (CASS − BK = 2.50), Pb^{2+} (CASS − BK = 1.57), and Cr^{total} (CASS − BK = 1.10). These results could evidence that cassava barks can be a more promising material in removing inorganic than organic contaminants. Moreover, our results evidence that CASS-BK is slower in adsorbing heavy metals. Chen et al. [46] found K_2 values (g mg^{-1} min^{-1}) ranging from 0.0017 to 0.0059 using modified corn cobs and chestnut shells for Pb^{2+} removal. In both cases, adsorption velocity is much lower than observed in this research.

3.2.3. Equilibrium Studies and Side-by-Side Comparison (Activated Carbon) and the Reusability of the Materials in Other New Adsorption Cycles. Table S8 and S9 exhibit the ANOVA results, while the isotherms and R^2 values are presented in Table 3 and Figure S4. The goodness of the fit obtained for Freundlich, Langmuir, Temkin and Pyzhev, Khan, Sips, Liu, and Redlich-Peterson suggest good predictions of those models on the observed adsorption phenomena.

(1) Cd^{2+} Equilibrium Studies. Langmuir predictions indicate a higher theoretical adsorption capacity ($q_{Langmuir}$, expressed in mg g^{-1}) for the AC (with $q_{Langmuir} = 21.49$), followed by CASS-Bk ($q_{Langmuir} = 16.03$), CASS-BB ($q_{Langmuir} = 14.81$), and CASS-BA ($q_{Langmuir} = 14.75$). Furthermore, $K_{Langmuir}$ values (expressed in L mg^{-1}) also indicate higher affinity between AC and Cd^{2+} than cassava-based adsorbents, with the following order: $K_{Langmuir\ AC}$ 0.57 > $K_{Langmuir\ CASS-BB}$ of 0.22 > $K_{Langmuir\ CASS-BK}$ of 0.13 > $K_{Langmuir\ CASS-BA}$ of 0.11. Thus, AC presented higher maximum adsorption capacity and affinity with Cd^{2+} than cassava adsorbents.

Similar behavior is seen in Freundlich parameters, with $K_{Frelundlich}$ (expressed in (mg g^{-1} (mg L^{-1})$^{-1/n}$)) presenting the following order: $K_{Freundlich\ AC}$ of 7.95 > $K_{Freundlich\ CASS-BB}$ of 4.96 > $K_{Freundlich\ CASS-BK}$ of 3.63 > $K_{Freundlich\ CASS-BA}$ of 3.31. Nevertheless, $n_{Freundlich\ CASS-BB}$ (3.76) > $n_{Freundlich\ AC}$ (3.18) indicates a higher adsorption intensity and a better distribution of the energy and heterogeneity of adsorbate sites [47] for CASS-BB against AC. Moreover, $n_{Freundlich}$ values are found between 1 and 10, and $1/n$ is between 0 and 1, indicating a favorable and cooperatively adsorption [48–50].

Sips, also known as the Langmuir-Freundlich model, can predict simultaneously mono and multilayer adsorption. For example, CASS-BK (65.38) and CASS-BB (131.82) presented higher q_{Sips} (expressed in mg g^{-1}) than AC (21.35), i.e., predicting that cassava-based adsorbents could remove more Cd^{2+} from water than AC in the evaluated physicochemical conditions. Nevertheless, K_{Sips} values show that AC possesses a higher affinity with Cd^{2+} than cassava-adsorbents ($K_{Sips\ AC} > K_{Sips\ CASSAVA-ADSORBENTS}$). Furthermore, the cassava adsorbents presented n_{Sips} lower than 0.6 (i.e., deviation from the unity), indicating higher proximity to the Freundlich model, while AC presented $n_{Sips} = 1.018$, suggesting higher similarity to the Langmuir assumptions [51].

The Redlich-Peterson model is similar to Sips, as it is a hybrid isotherm model that features Freundlich and Langmuir isotherm models with three parameters [52]. It approaches the Freundlich model at high concentration (as $\beta_{RP} \to 0$) and at low concentration to Langmuir isotherm (as $\beta_{RP} \to 1$) [53]. The values of β_{RP} follow the order:

Table 2: Kinetic parameters for the adsorption of Cd^{2+}, Pb^{2+}, and Cr^{total} by CASS-BK, CASS-BA, and CASS-BB, using the nonlinear models of pseudofirst order (PFO) and pseudosecond order (PSO).

Kinetic parameters		Cd^{2+}			Pb^{2+}			Cr^{total}	
PFO	CASS-BK	CASS-BA	CASS-BB	CASS-BK	CASS-BA	CASS-BB	CASS-BK	CASS-BA	CASS-BB
k_1 (min^{-1})	1.1928 ± 0.0026	1.2077 ± 0.0025	$1.2425 \pm 6.8616 \cdot 10^{-4}$	1.1453 ± 0.0063	1.2252 ± 0.0035	1.2308 ± 0.0038	1.0327 ± 0.0035	1.1601 ± 0.0050	1.1706 ± 0.0011
q_e cal. ($mg\,g^{-1}$)	0.5598 ± 0.0235	0.5656 ± 0.0229	0.8022 ± 0.0202	0.5313 ± 0.0517	0.5560 ± 0.0301	0.6789 ± 0.0619	0.6813 ± 0.0691	0.5870 ± 0.0536	0.8863 ± 0.0544
Reduced Chi^2	$6.6307\ 10^{-5}$	$6.08439\ 10^{-5}$	$4.6745\ 10^{-6}$	0.0004	0.0002	0.0001	0.0001	0.0002	$1.2741\ 10^{-5}$
R-square (COD)	1.000	1.000	1.000	0.9967	1.000	0.9989	0.9987	1.000	0.9999
Adj. R^2	1.000	1.000	1.000	0.9964	1.000	0.9988	0.9986	1.000	0.9999
PSO	CASS-BK	CASS-BA	CASS-BB	CASS-BK	CASS-BA	CASS-BB	CASS-BK	CASS-BA	CASS-BB
k_2 ($g\,mg^{-1}\,min^{-1}$)	2.5019 ± 0.1252	2.5443 ± 0.1151	8.4765 ± 0.4883	1.8871 ± 0.1918	2.3549 ± 0.1940	3.8177 ± 0.6579	4.2999 ± 0.7287	2.4666 ± 0.2611	11.4556 ± 1.3146
q_e cal. ($mg\,g^{-1}$)	1.2012 ± 0.0012	1.2161 ± 0.0011	$1.2451 \pm 4.5838 \cdot 10^{-4}$	1.1577 ± 0.0032	1.2342 ± 0.0022	1.2372 ± 0.0029	1.0385 ± 0.0025	1.1698 ± 0.0027	$1.1728 \pm 6.8020 \cdot 10^{-4}$
Reduced Chi^2	$1.1189\ 10^{-5}$	$8.9005\ 10^{-6}$	$1.5372\ 10^{-6}$	$7.4262\ 10^{-5}$	$3.3954\ 10^{-5}$	$6.2170\ 10^{-5}$	$4.6976\ 10^{-5}$	$5.1007\ 10^{-5}$	$3.3913\ 10^{-6}$
R-square (COD)	0.9999	0.9999	0.9999	0.9994	0.9997	0.9995	0.9995	0.9996	0.9999
Adj. R^2	0.9999	0.9999	0.9999	0.9993	0.9997	0.9995	0.9995	0.9995	0.9999
q_e exp. ($mg\,g^{-1}$)	1.1858 ± 0.022	1.2009 ± 0.022	1.2404 ± 0.007	1.1375 ± 0.030	1.2178 ± 0.025	1.2267 ± 0.017	1.0295 ± 0.015	1.1542 ± 0.024	1.1694 ± 0.005

Notes: q_e calc. and exp., respectively, the amount of metal adsorbed estimated by the model and obtained experimentally. k_1: rate constant of pseudofirst order; k_2: rate constant of pseudosecond order; A: constant indicating the initial chemisorption rate; B: number of suitable sites for adsorption, related to the extent of surface coverage and the activation energy of the chemo reaction; Reduced Chi^2: residual sum of squares; R-square (COD): coefficient of determination; Adj R^2: adjusted coefficient of determination.

Table 3: Equilibrium parameters by the nonlinear models of Langmuir, Freundlich, Sips, Redlich-Peterson, Toth, Temkin, Liu, and Khan to remove Cd^{2+}, Pb^{2+}, and Cr^{total} by cassava-based adsorbents.

Parameters		Cd^{2+}				Pb^{2+}			Cr^{total}			
		CASS-BK	CASS-BA	CASS-BB	AC	CASS-BK	CASS-BA	CASS-BB	CASS-BK	CASS-BA	CASS-BB	AC
Langmuir	$q_{Langmuir}$ (mg g^{-1})	16.03158 ± 1.36538	14.74882 ± 0.86014	14.80667 ± 1.25349	21.49443 ± 0.53588	30.09417 ± 2.31339	25.25276 ± 1.24648	23.44436 ± 1, 43539	18.3884 ± 2.01416	14.09721 ± 0.79578	13.28135 ± 0.38244	12.80244 ± 0.36463
	$K_{Langmuir}$ (L mg^{-1})	0.13825 ± 0.04738	0.11403 ± 0.02594	0.21865 ± 0.09085	0.57279 ± 0.04805	0.20149 ± 0.0351	0.52968 ± 0.07527	1.06964 ± 0.21915	0.04017 ± 0.0106	0.04855 ± 0.00811	0.08824 ± 0.00918	0.84959 ± 0.14625
	$R_{Langmuir}$ (5 to 200 mg L^{-1})	0.035 to 0.591	0.042 to 0.637	0.022 to 0.478	0.009 to 0.259	0.024 to 0.498	0.009 to 0.274	0.005 to 0.158	0.111 to 0.833	0.093 to 0.805	0.054 to 0.694	0.006 to 0.191
	Reduced Chi^2	2.04954	0.82442	2.65031	0.3994	1.11639	1.10101	2.32819	1.28388	0.33446	0.15877	0.51943
	R-square (COD)	0.93203	0.96577	0.90632	0.99261	0.98171	0.98234	0.9635	0.94969	0.98036	0.99129	0.97845
	Adj. R^2	0.9235	0.96149	0.89461	0.99169	0.97942	0.98013	0.95894	0.9434	0.97791	0.9902	0.97575
Freundlich	$K_{freundlich}$ (mg g^{-1} (mg $L^{-1})^{-1/n}$)	3.63599 ± 0.28729	3.30651 ± 0.24546	4.96969 ± 0.18872	7.95208 ± 0.91248	5.78945 ± 0.51863	8.40103 ± 0.70876	10.32826 ± 0.73736	1.90101 ± 0.6364	1.94262 ± 0.38241	2.68319 ± 0.51933	5.69459 ± 0.62652
	$n_{Freundlich}$ (dimensionless)	2.80628 ± 0.17702	2.93935 ± 0.17473	3.76663 ± 0.15428	3.17685 ± 0.46251	1.84867 ± 0.14726	2.35796 ± 0.24608	2.65845 ± 0.29211	2.15719 ± 0.41389	2.47454 ± 0.30651	2.90776 ± 0.42751	4.70953 ± 0.6928
	$1/n_{Freundlich}$ (dimensionless)	0.3563	0.3402	0.2655	0.315	0.5409	0.4241	0.3762	0.4636	0.4041	0.3439	0.2123
	Reduced Chi^2	0.42388	0.30506	0.1459	5.8525	1.71008	3.34026	3.71903	3.81642	0.96709	1.54048	2.06817
	R-square (COD)	0.98594	0.98733	0.99484	0.89173	0.97198	0.94641	0.9417	0.85045	0.94322	0.9155	0.91419
	Adj. R^2	0.98418	0.98575	0.9942	0.8782	0.96848	0.93971	0.93441	0.83175	0.93612	0.90493	0.90346
Sips	q_{Sips} (mg g^{-1})	65.38617 ± 81.16848	25.39482 ± 4.38679	131.82648 ± 247.93561	21.35258 ± 0.87117	37.41387 ± 10.90253	27.79766 ± 5.07839	26.99272 ± 3.36206	14.7634 ± 1.23577	14.79742 ± 2.13484	13.20523 ± 0.74521	14.00721 ± 0.55321
	K_{Sips} (L mg^{-1})	9.83687 10 − 4 ± 0.00441	0.01926 ± 0.01263	1.13984 10 − 5 ± 9.6380 10 − 5	0.58341 ± 0.07056	0.12015 ± 0.08481	0.63578 ± 0.37545	0.44236 ± 0.15258	0.05997 ± 0.009	0.04348 ± 0.01608	0.08935 ± 0.01365	0.62075 ± 0.11802
	n_{Sips}	0.41406 ± 0.09095	0.52448 ± 0.05307	0.28496 ± 0.04239	1.01783 ± 0.09192	0.84556 ± 0.15122	0.76903 ± 0.16365	0.90902 ± 0.14204	1.59095 ± 0.28295	0.92013 ± 0.1756	1.01434 ± 0.11589	0.69058 ± 0.0708
	Reduced Chi^2	0.45231	0.10491	0.16054	0.45392	1.1103	2.16475	1.19517	0.73073	0.37173	0.18103	0.20415
	R-square (COD)	0.98687	0.99619	0.99503	0.99265	0.98408	0.97031	0.98322	0.97494	0.9809	0.99131	0.99259
	Adj. R^2	0.98312	0.9951	0.99362	0.99055	0.97953	0.96182	0.97843	0.96779	0.97545	0.98883	0.99047
Redlich-Peterson	K_{RP} (L g^{-1})	16.70571 ± 12.37434	8.36071 ± 2.54453	283.25074 ± 224.62529	13.26416 ± 1.67146	8.32751 ± 2.94818	38.72759 ± 14.2866	16.7139 ± 4.08174	0.43367 ± 0.02326	0.59042 ± 0.14514	1.01102 ± 0.14273	18.64749 ± 3.19075
	a_{RP} (L mg^{-1})	3.72107 ± 3.25994	1.84552 ± 0.71026	54.4878 ± 44.66023	0.67642 ± 0.16112	0.52827 ± 0.43438	2.3358 ± 1.27182	0.89245 ± 0.41738	2.29001 10^{-4} ± 2.1952 · 10^{-4}	0.02661 ± 0.02844	0.05474 ± 0.02478	2.01019 ± 0.45332
	⊠$_{RP}$ (dimensionless)	0.69553 ± 0.03834	0.73312 ± 0.02143	0.74687 ± 0.01166	0.96965 ± 0.03829	0.77516 ± 0.15977	0.83509 ± 0.0845	0.87888 ± 0.09025	2.01047 ± 0.19961	1.09409 ± 0.17562	1.07179 ± 0.07031	0.91411 ± 0.01727
	Reduced Chi^2	0.32188	0.07992	0.10797	0.41509	0.97008	1.72126	0.97036	0.17667	0.37164	0.15871	0.14841
	R-square (COD)	0.99066	0.9971	0.99666	0.99328	0.98609	0.97639	0.98638	0.99394	0.98091	0.99238	0.99461
	Adj. R^2	0.98799	0.99627	0.99571	0.99136	0.98212	0.96964	0.98249	0.99221	0.97545	0.99021	0.99307
Toth	q_{Toth} (mg g^{-1})	392.17758 ± 1418.39671	46.32464 ± 19.32673	61269.30629 ± 1.07973*E6*	21.76049 ± 1.15496	47.44475 ± 28.74734	31.47671 ± 9.72964	29.51154 ± 6.0196	13.34476 ± 0.52064	14.23303 ± 2.60567	12.92332 ± 0.85817	14.62388 ± 0.75137
	b_t (dimensionless)	17.79585 ± 93.2196	1.14213 ± 0.86741	1.83899*E*11 ± 1.07978*E*13	0.59026 ± 0.09258	0.19285 ± 0.04945	1.57452 ± 0.77771	0.59327 ± 0.14267	0.02969 ± 0.00183	0.04924 ± 0.01337	0.08228 ± 0.01424	2.29449 ± 0.81443
	n_{Toth} (dimensionless)	0.11468 ± 0.10939	0.24313 ± 0.06156	0.0355 ± 0.07232	0.95864 ± 0.1546	0.60065 ± 0.30642	0.56938 ± 0.24045	0.74607 ± 0.23928	5.35184 ± 2.51761	0.97637 ± 0.38958	1.09872 ± 0.23239	0.54805 ± 0.07842
	Reduced Chi^2	0.41282	0.08771	0.05805	0.45161	1.02201	1.96881	1.0885	0.33913	0.38211	0.17679	0.16318
	R-square (COD)	0.98802	0.99681	0.99994	0.99269	0.98535	0.97299	0.98472	0.98837	0.98037	0.99151	0.99408
	Adj. R^2	0.9846	0.9959	0.99992	0.9906	0.98116	0.96528	0.98035	0.98505	0.97476	0.98909	0.99238
Temkin and Pyzhev	b_{TP} (dimensionless)	1.00569 ± 0.07297	1.14545 ± 0.08256	1.5761 ± 0.15064	0.61398 ± 0.02149	0.44159 ± 0.02692	0.54628 ± 0.02374	0.4846 ± 0.00996	0.63938 ± 0.05938	1.05262 ± 0.0929	1.02271 ± 0.06056	1.37757 ± 0.05278
	A_{TP} (L mg^{-1})	5.19005 ± 1.53976	5.19616 ± 1.6121	74.10073 ± 44.81592	7.75829 ± 0.84755	3.06553 ± 0.43124	14.36746 ± 1.82544	6.45312 ± 0.34133	0.44175 ± 0.09563	1.17421 ± 0.34885	1.5298 ± 0.3132	28.33647 ± 5.84206
	Reduced Chi^2	1.20705	0.95169	1.90872	0.51953	1.74482	0.94036	0.20794	1.63193	0.98971	0.49258	0.27695
	R-square (COD)	0.95997	0.96048	0.93253	0.99039	0.97141	0.98526	0.99666	0.93605	0.94189	0.97298	0.98851
	Adj. R^2	0.95496	0.95554	0.9241	0.98919	0.96784	0.98342	0.99625	0.92806	0.93463	0.9696	0.98707
Liu	q_{Liu} (mg g^{-1})	65.38617 ± 81.16848	25.39482 ± 4.38679	131.82648 ± 247.93561	21.35258 ± 0.87117	37.41387 ± 10.90253	27.79766 ± 5.07839	26.99272 ± 3.36206	14.7634 ± 1.23577	14.79742 ± 2.13484	13.20523 ± 0.74521	14.00721 ± 0.55321
	k_g (L mg^{-1})	9.83687 10 − 4 ± 0.00441	0.01926 ± 0.01263	1.13984 10^{-5} ± 9.6380 10^{-5}	0.58341 ± 0.07056	0.12015 ± 0.08481	0.63578 ± 0.37545	0.44236 ± 0.15258	0.05997 ± 0.009	0.04348 ± 0.01608	0.08935 ± 0.01365	0.62075 ± 0.11802
	n_{Liu} (dimensionless)	0.41406 ± 0.09095	0.52448 ± 0.05307	0.28496 ± 0.04239	1.01783 ± 0.09192	0.84556 ± 0.15122	0.76903 ± 0.16365	0.90902 ± 0.14204	1.59095 ± 0.28295	0.92013 ± 0.1756	1.01434 ± 0.11589	0.69058 ± 0.0708
	Reduced Chi^2	0.45231	0.10491	0.16054	0.45392	1.1103	2.16475	1.19517	0.73073	0.37173	0.18103	0.20415
	R-square (COD)	0.98687	0.99619	0.99503	0.99265	0.98408	0.97031	0.98322	0.97494	0.9809	0.99131	0.99259
	Adj. R^2	0.98312	0.9951	0.99362	0.99055	0.97953	0.96182	0.97843	0.96779	0.97545	0.98883	0.99047

Table 3: Continued.

Parameters		CASS-BK	CASS-BA	CASS-BB	AC	CASS-BK	CASS-BA	CASS-BB	CASS-BK	CASS-BA	CASS-BB	AC
				Cd^{2+}			Pb^{2+}			Cr^{total}		
Khan	q_{Khan} (mg g^{-1})	2.79776 ± 1.09417	3.39747 ± 0.65966	1.58272 ± 0.4133	18.78451 ± 2.71831	11.86292 ± 7.7197	11.6408 ± 4.5597	15.33791 ± 5.38731	308383.429 ± 6.50488 10^8	23.82914 ± 14.28871	17.93275 ± 3.93123	8.38776 ± 0.85235
	b_{Khan} (L mg^{-1})	3.66843 ± 3.1002	1.86396 ± 0.79712	103.28289 ± 86.05213	0.70103 ± 0.16585	0.64488 ± 0.5585	3.01044 ± 1.93491	1.04077 ± 0.53624	1.75541 10^{-6} ± 0.0037	0.02429 ± 0.01851	0.05697 ± 0.01811	2.0356 ± 0.49317
	a_{Khan} (dimensionless)	0.68337 ± 0.0296	0.71157 ± 0.01807	0.74516 ± 0.01046	0.95377 ± 0.04581	0.66711 ± 0.14614	0.79328 ± 0.08209	0.82211 ± 0.09717	8129.76185 ± 1.7233 107	1.31273 ± 0.46136	1.14086 ± 0.11927	0.90671 ± 0.01841
	Reduced Chi^2	0.27699	0.08228	0.0955	0.39659	0.91343	1.60777	0.89426	0.25455	0.35402	0.14764	0.15629
	R-square (COD)	0.99196	0.99701	0.99705	0.99358	0.9869	0.97795	0.98745	0.99127	0.98181	0.99291	0.99433
	Adj. R^2	0.98967	0.99616	0.9962	0.99175	0.98316	0.97165	0.98386	0.98878	0.97662	0.99089	0.9927

Notes: it was impossible to construct an isotherm for the comparison study of Pb^{2+} with activated carbon (AC).

β_{RP-AC} (0.969) > $\beta_{RP\text{CASS-BB}}$ (0.744) > $\beta_{RP\text{CASS-BA}}$ (0.733) > $\beta_{RP\text{CASS-BK}}$ (0.695). As evidenced above, n_{Sips} assumes values inferior but closer to the unity (exception for AC, with β_{RP} > 1), indicating certain proximity with the Langmuir monolayer model.

The b_{TP} values (dimensionless) obtained by the Temkin model follow the order: $b_{\text{TP BB}}$ (1.57) > $b_{\text{TP CASS–BA}}$ (1.14) > $b_{\text{TP CASS–BK}}$ (1.00) > $b_{\text{TP AC}}$ (0.61), which could be assigned to the more vital interaction between Cd^{2+} ions and active sites of the cassava adsorbents when compared to AC [54].

Liu's model is derived from a combination of Langmuir and Freundlich models; thus, the Langmuir assumption of the monolayer formation and the Freundlich infinite adsorption assumption are eliminated by the Liu model [55]. This model predicts that active adsorbent sites cannot have the same energy, and its often used for better predictions of Liu's maximum adsorption capacity prediction (q_{Liu}). The q_{Liu} (mg g^{-1}) predicts the following order: $q_{\text{Liu CASS–BB}}$ (131.82) > $q_{\text{Liu CASS–BK}}$ (65.38) > $q_{\text{Liu CASS–BA}}$ (25.39) > $q_{\text{Liu CASS–AC}}$ (21.35), suggesting higher removal of Cd^{2+} by the cassava-adsorbents than AC.

Khan's predictions on Cd^{2+} maximum adsorption capacity (q_{Khan}, expressed in mg g^{-1}) followed the order: $q_{\text{Khan AC}}$ (18.78) > $q_{\text{Khan BB}}$ (3.98) > $q_{\text{Khan BA}}$ (3.39) > $q_{\text{Khan BK}}$ (2.79), indicating superiority of AC in Cd^{2+} removal. When the a_{Khan} exponent equals 1, Khan isotherm approaches Langmuir monolayer interpretation [56], as observed for a_{Khan} AC = 0.953, but not for cassava adsorbents, with 0.68 < $a_{\text{Khan adsorbents}}$ < 0.74.

(2) Pb^{2+} Equilibrium Studies. CASS-BK presented the highest Pb^{2+} adsorption maximum capacity (q_{Langmuir} = 30.09 mg g^{-1}), followed by CASS-BA (q_{Langmuir} = 25.25 mg g^{-1}), and CASS-BB (q_{Langmuir} = 23.44 mg g^{-1}). Nevertheless, CASS-BB presented the highest K_{Langmuir} values despite lower maximum adsorption capacity, indicating a higher affinity between Pb^{2+} and CASS-BB against other cassava adsorbents.

$K_{\text{Freundlich}}$ values ((mg g^{-1} (mg L^{-1})$^{-1/n}$)) indicate a higher affinity of CASS-BB with Pb^{2+} ($K_{\text{Freundlich CASS–BB}}$ = 10.32), than CASS-BA ($K_{\text{Freundlich CASS–BA}}$ = 8.40), and CASS-BK ($K_{\text{Freundlich CASS–BK}}$ = 5.79). Moreover, $n_{\text{Freundlich}}$ values suggest the same order for Pb^{2+} adsorption intensity CASS − BB > CASS − BA > CASS − BK.

The maximum capacity of Pb^{2+} adsorption predicted by Sips (expressed in mg g^{-1}) followed the order: $q_{\text{Sips CASS–BK}}$ of 37.41 > $q_{\text{Sips CASS–BB}}$ of 27.79 > $q_{\text{Sips CASS–BA}}$ of 26.99. n_{Sips} values are lower than 1 (0.12 < q_{Sips} < 0.63), suggesting proximity with Freundlich multilayer assumptions. K_{Sips} (L mg^{-1}) values indicate the following order of affinity with Pb^{2+}: $K_{\text{Sips CASS–BA}}$ of 0.63 > $K_{\text{Sips CASS–BB}}$ of 0.44 > $K_{\text{Sips BK}}$ of 0.12.

Using activated carbon (AC) from tobacco wastes for the removal of Pb^{2+}, [40] found q_{Langmuir} = 71.573 mg g^{-1}, $K_{\text{Freundlich}}$ = 76.076 ((mg g^{-1} (mg L^{-1})$^{-1/n}$)), and q_{Sips} = 155.440 (mg g^{-1}), i.e., higher than the observed for cassava-based adsorbents. Nevertheless, it is important to consider the enhanced characteristics of an AC compared to an unmodified adsorbent. Furthermore, although the lower adsorption performance, cassava adsorbents have the advantage of easy obtaining and low cost of production.

K_{RP} (L g^{-1}) values followed the order: $K_{\text{RP CASS–BA}}$ of 38.72 > $K_{\text{RP CASS–BB}}$ of 16.71 > $K_{\text{RP CASS–BK}}$ of 8.32, while β_{RP} values follow the order: $\beta_{RP\text{BB}}$ of 0.878 > $\beta_{RP\text{CASS–BA}}$ of 0.835 > $\beta_{RP\text{CASS–BK}}$ of 0.775, i.e., inferior but closer to 1, indicating proximity to the Langmuir model. Temkin b_{TP} values follow the order: $b_{\text{TP CASS–BA}}$ of 0.54 > $b_{\text{TP CASS–BB}}$ of 0.48 > $b_{\text{TP CASS–BK}}$ of 0.44, suggesting a higher interaction between Pb^{2+} and CASS-BA than CASS-BK [54]. The q_{Liu} (mg g^{-1}) obtained for Pb^{2+} removal predicts the following order: $q_{\text{Liu CASS–BK}}$ of 37.38 > $q_{\text{Liu CASS–BA}}$ of 27.78 > $q_{\text{Liu CASS–BB}}$ of 26.98, suggesting higher removal of Pb^{2+} by CASS-BK than CASS-BB [55].

The following order is observed for q_{Khan} parameter (q_{Khan}, expressed in mg g^{-1}): $q_{\text{Khan CASS–BB}}$ of 15.33 > $q_{\text{Khan CASS–BK}}$ of 11.86 > $q_{\text{Khan CASS–BA}}$ of 11.64, indicating a higher adsorption capacity prediction for CASS-BB. Furthermore, similar to Cd^{2+} adsorption, a_{Khan} exponent was distant from the unity, suggesting more excellent proximity to Freundlich assumptions [56].

(3) Cr^{total} Equilibrium Studies. Langmuir model predicted the following values for maximum Cr^{total} adsorption (q_{Langmuir}, expressed in mg g^{-1}): $q_{\text{Langmuir CASS-BK}}$ (18.38) > $q_{\text{Langmuir CASS-BA}}$ (14.09) > $q_{\text{Langmuir CASS-BB}}$ (13.28) > $q_{\text{Langmuir AC}}$ (12.80), illustrating a superiority of cassava adsorbents compared to AC. Furthermore, K_{Langmuir} values demonstrate that CASS-BB is as good as AC regarding chemical affinity with Cr^{total}, with the higher $K_{\text{Langmuir CASS–BB}}$ (0.882) > $K_{\text{Langmuir CASS–AC}}$ (0.849) > $K_{\text{Langmuir CASS–BA}}$ (0.048) > $K_{\text{Langmuir CASS–BK}}$ (0.040).

Nevertheless, $K_{\text{Freundlich}}$ ((mg g^{-1} (mg L^{-1})$^{-1/n}$)) predict a higher affinity of AC–Cr^{total} adsorption: $K_{\text{Freundlich AC}}$ (5.69) > $K_{\text{Freundlich CASS–BB}}$ (2.68) > $K_{\text{Freundlich CASS–BA}}$ (1.94) > $K_{\text{Freundlich CASS–BK}}$ (1.90). Similarly, in Cd^{2+} and Pb^{2+} adsorption studies, $n_{\text{Freundlich}}$ presented values within 1 and 10, and $1/n_{\text{Freundlich}}$ between 0 and 1 (2.15 < $n_{\text{Freundlich}}$ < 4.71 ; 0.21 < $1/n_{\text{Freundlich}}$ < 0.46), suggesting a favorable and cooperatively adsorption system [48–50].

q_{Sips} (mg g^{-1}) shows a consistent behavior, with certain proximity between the Cr^{total} maximum adsorption capacities, and a slight advantage for CASS-BA against AC: $q_{\text{Sips CASS–BA}}$ (14.79) > $q_{\text{Sips CASS–BK}}$ (14.76) > $q_{\text{Sips CASS–AC}}$ (14.00) > $q_{\text{Sips CASS–BB}}$ (13.20). Furthermore, n_{Sips} < 1 suggests proximity to Freundlich assumptions for CASS-BK (n_{Sips} = 0.91) and AC (n_{Sips} = 0.69), while a proximity to Langmuir is observed for CASS-BK (n_{Sips} = 1.87) and CASS-BB (n_{Sips} = 1.01).

The Redlich-Peterson exponent (β_{RP}) presented the following values: β_{RP}CASS − BK = 2.01 > β_{RP}CASS − BA = 1.09 > β_{RP}CASS − BA = 1.07 > β_{RP}CASS − AC = 0.91, i.e., cassava adsorbents are mostly $\beta_{RP} \rightarrow 1$, suggesting proximity to the Langmuir model, while the opposite is observed for AC.

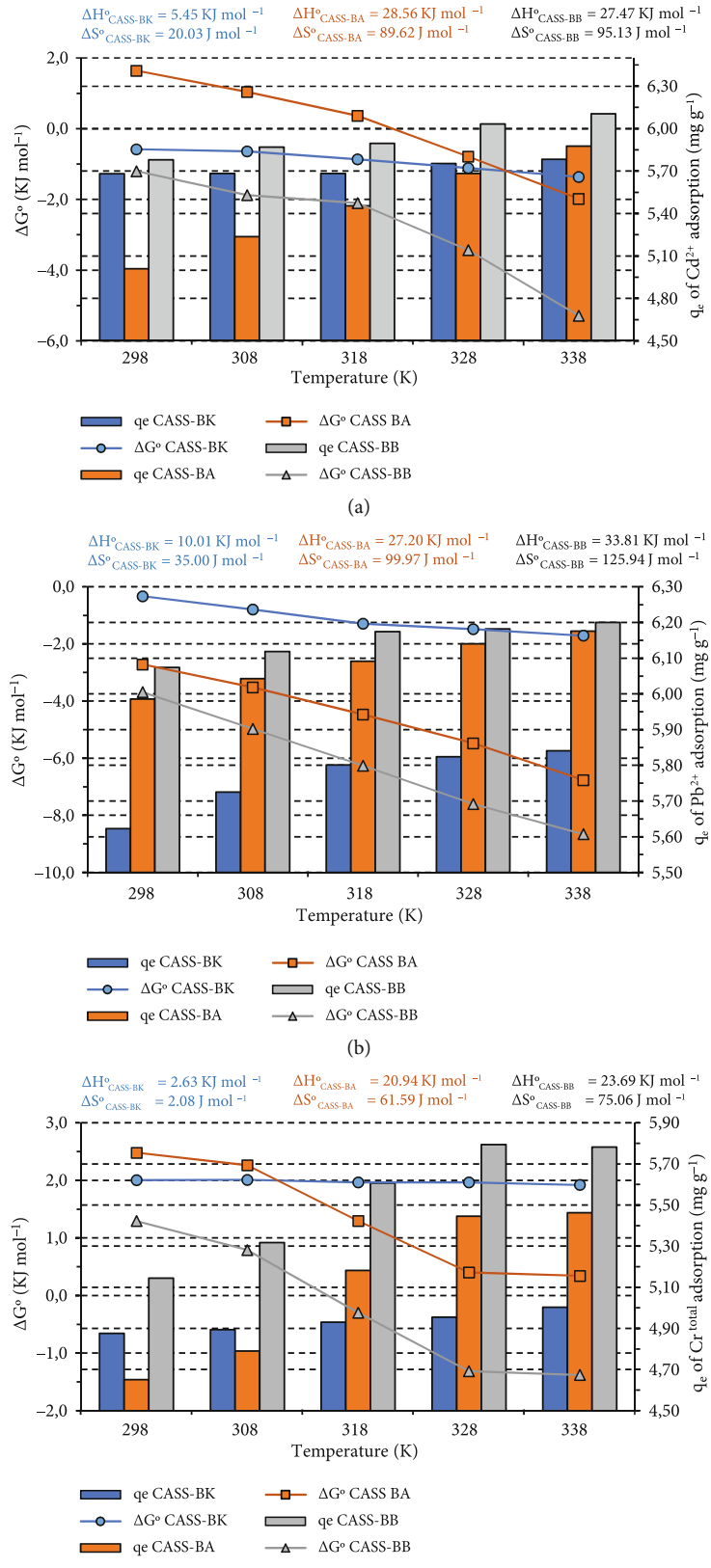

FIGURE 6: Thermodynamic parameters obtained in the adsorption of Cd^{2+} (a), Pb^{2+} (b), and Cr^{total} (c) by CASS-BK, CASS-BA, and CASS-BB. Experimental conditions: adsorbent dose of 8.0 g L^{-1}, pH of 5.5, stirring at 160 rpm for 60 min, C_0 of Cd^{2+}, Pb^{2+}, and Cr^{total} = 50, 100, and 50 mg L^{-1}.

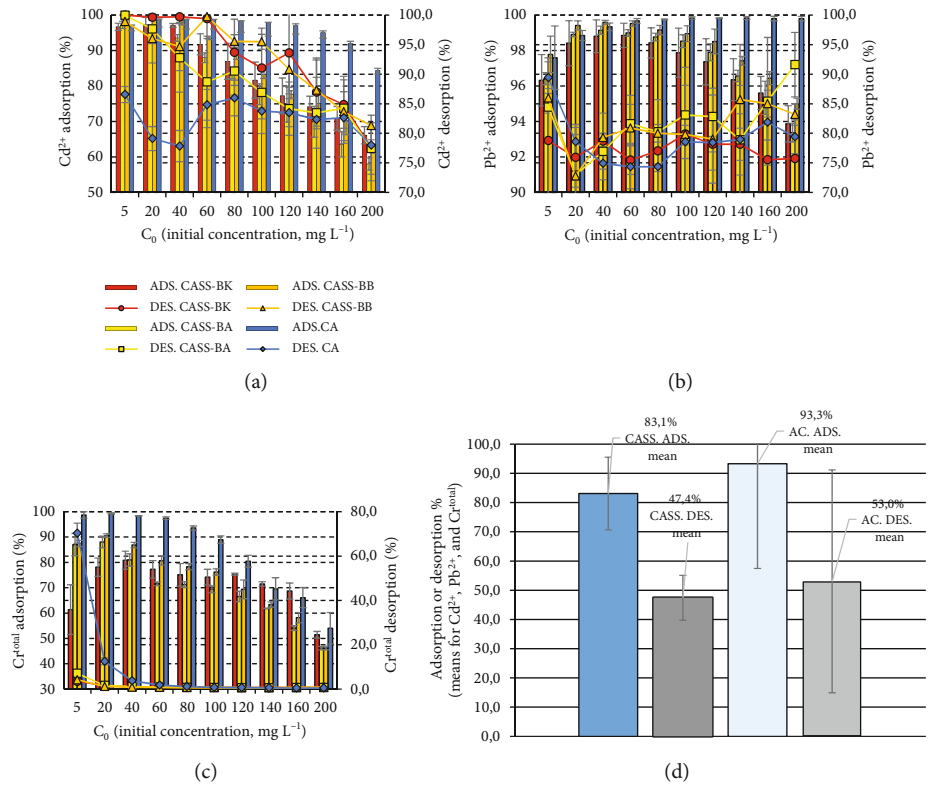

Figure 7: Cd^{2+} (a), Pb^{2+} (b), and Cr^{total} (c) adsorption (ADS) and desorption (DES) percentage for CASS-BK, CASS-BA, and CASS-BB, in different initial concentrations (from 5.0 to 200 mg L^{-1}). Mean for the adsorption and desorption of 3 heavy metals (d). Experimental conditions: adsorbent dose of 8.0 g L^{-1}, pH of 5.5, stirring at 160 rpm for 60 min, at 298 K.

For Cr^{total} adsorption, b_{TP} values follow the order: $b_{TP\,CASS-AC}$ (1.37) > $b_{TP\,CASS-BA}$ (1.05) > $b_{TP\,CASS-BB}$ (1.022) > $b_{TP\,CASS-BK}$ (0.64). Thus, indicating higher interaction between Cr^{total} and AC than the cassava adsorbents. It is essential to highlight that CASS-BK presented the higher values of b_{TP} for Pb^{2+} but had the lowest values for Cr^{total} adsorption.

The maximum adsorption of Cr^{total} predicted by the Liu model indicates the following order: $q_{Liu\,CASS-BA}$ (14.80) > $q_{Liu\,CASS-BK}$ (14.76) > $q_{Liu\,CASS-AC}$ (14.00) > $q_{Liu\,CASS-BB}$ (13.20), highlighting a superiority of CASS-BA against AC.

q_{Khan} shows maximum adsorption capacity predictions for Cr^{total} in the following order: $q_{Khan\,CASS-BA}$ (23.82) > $q_{Khan\,BB}$ (17.93) > $q_{Khan\,CASS-AC}$ (8.39). It is essential to state that the results of CASS-BK were overestimated. Nevertheless, the results suggest the superiority of CASS-BA and CASS-BB against AC in Cr^{total} adsorption. Furthermore, a_{Khan} exponent was superior to 1 for CASS-BA and CASS-BB, suggesting proximity to Langmuir assumptions, while for AC $a_{Khan} < 1$, suggesting higher Freundlich proximity [56].

3.2.4. The Effect of Temperature on Cd^{2+}, Pb^{2+}, and Cr^{total} adsorption by the Cassava Adsorbents. The effect of temperature on heavy metal adsorption is shown in Figure 6, with q_e values increasing with temperature rise. On the other hand, entropy, enthalpy, and Gibbs's free energy decrease with temperature increase.

For Cd^{2+} adsorption, $\Delta H°$ (kJ mol^{-1}) values followed the order: CASS.BA (28.56) > CASS.BB (27.47) > CASS.BK (5.56); for Pb^{2+} adsorption : CASS.BB (33.81) > CASS.BA (27.20) > CASS.BK (−10.01), while for Cr^{total} adsorption: CASS.BB (2.63) > CASS.BA (20.94) > CASS.BK (23.69). Therefore, only CASS.BK presented exothermic adsorption of Pb^{2+}, while the other studied cases the heavy metal adsorption is endothermic.

For Cd^{2+} adsorption, $\Delta S°$ (J mol^{-1}) values assumed the following order: CASS.BB (95.13) > CASS.BA (89.62) > CASS.BK (20.03), for Pb^{2+} adsorption: CASS.BB (125.94) > CASS.BA (99.98) > CASS BK (35.00), while for Cr^{total} adsorption: CASS.BB (75.06) > CASS.BA (61.59) > CASS. BK (2.08). Therefore, higher randomness is observed using the bagasse of cassava (BA) or its mixture with barks (BB) when compared to cassava barks (BK).

3.2.5. Heavy Metal Removal by Cassava-Based Adsorbents and Desorption Studies—General Considerations, the Summary of Our Findings. Figure 7(d) shows 83% of adsorption of heavy metals (Cd^{2+}, Pb^{2+}, and Cr^{total}) by the cassava-based materials, with a 47% rate of desorption. On the other hand, the AC presented 93% adsorption with a 53% desorption rate. In other words, AC presented higher adsorption and desorption of heavy metals. Nevertheless, cassava-based adsorbents presented close results, highlighting their great potential.

Wu et al. [45] removed 96% of Rhodamine B using cassava slag biochar. Guo et al. [57] removed 99% of Cr (IV) using cassava sludge-based AC. Chen et al. [46] reached 79% and 86% of Pb^{2+} removal using modified corn cobs

and chestnut shells. Scheufele et al. [58] removed 60% of direct black dye using cassava root husks. As observed, cassava-based adsorbents and their derivatives still have great potential for removing organic and inorganic contaminants from water mediums.

As mentioned above, the adsorption means obtained during the equilibrium studies highlight the great potential of cassava-adsorbents removing heavy metals, such as Cd^{2+}, Pb^{2+}, and Cr^{total} from water. CASS-BK removed on average 83.98% of Cd^{2+}, 96.06% of Pb^{2+}, and 65.65% of Cr^{total}; CASS-BA removed 80.27% of Cd^{2+}, 97.36% of Pb^{2+}, and 67.76% of Cr^{total}; CASS-BB removed 84.91% of Cd^{2+}, 98.18% of Pb^{2+}, and 73.72% of Cr^{total} (Figure 7); meanwhile, the AC, a commercial adsorbent removed 95.74% of Cd^{2+}, 99.43% of Pb^{2+}, and 84.65% of Cr^{total}. Thus, considering the averages obtained for the removal of heavy metal combined, cassava-adsorbents presented $83.10\% \pm 12.44$ of removal, against $93.27\% \pm 7.69$ from AC. Therefore, cassava-based adsorbents are competitive alternatives, especially considering their high availability and low cost.

The acid elution with HCl 0.1 M recovered a significant part of Cd^{2+} and Pb^{2+}, but only a fraction of Cr^{total} adsorbed by cassava materials. The desorption procedure was able to recover, on average, 63.22% of Cd^{2+}, 77.34% of Pb^{2+}, and only 1.18% of Cr^{total}. CASS-BA recovered 56.49% of Cd^{2+}, 81.80% of Pb^{2+}, and 0.85% of Cr^{total}. CASS-BB recovered 63.62% of Cd^{2+}, 81.17% of Pb^{2+}, and 1.14% of Cr^{total}. In contrast to the adsorbents, AC recovered 71.01% of Cd^{2+}, 78.88% of Pb^{2+}, and 9.26% of Cr^{total}.

Considering the excellent recovery rates obtained for Cd^{2+} and Pb^{2+}, it is possible to predict the reuse of cassava adsorbents in more than one adsorption cycle. Nevertheless, the same cannot be stated for Cr^{total} adsorption.

Compared to the obtained results, Manfrin et al., [59], using tobacco-activated carbon, achieved $q_{Langmuir} = 71.42\ mg\,g^{-1}$ of Pb^{2+}, Conradi Junior et al. [3] using tobacco activated carbon reached $q_{Langmuir} = 84.74\ mg\,g^{-1}$ of Pb^{2+}. Thus, superior values than $30.0\ mg\,g^{-1}$ were predicted by using CASS-BK. However, the cassava-based materials are adsorbents without modification, implying lower production costs. The low cost and considerably efficient removal are interesting for adopting this technology in industries wastewater treatments.

Barka et al. [60] reached $q_{Langmuir} = 54.05\ mg\,g^{-1}$ of Cd^{2+} using *Scolymus hispanicus* L. adsorbents, against $16.03\ mg\,g^{-1}$ of CASS-BK or [57] that reached $q_{Langmuir} = 9.84\ mg\,g^{-1}$ of Cr(IV) using cassava sludge-based activated carbon, against $18.38\ mg\,g^{-1}$ using CASS-BK. Thus, cassava-based adsorbents are still competitive with other unmodified and modified cellulose-based materials described in the literature. Therefore, their use in the adsorption of heavy metals is an exciting option.

4. Conclusion

SEM analysis reveals a heterogeneous structure full of cavities. In addition, FTIR before and after adsorption reveals gaps related to missing functional groups, suggesting a significant role of alkenes, carboxylic acid, alcohol, anhydride, and ether. pH_{PZC} is found at pH 6.02, 6.04, and 6.26, indicating a negatively charged surface above such points, which could potentiate cation adsorption.

In low concentrations of metals, the adsorbents derived from barks, bagasse, and their mixture better perform at pH 7.0 (94.9%) using $16\ g\,L^{-1}$ of adsorbents. Nevertheless, the most cost-benefit dose is found using $8.0\ g\,L^{-1}$, with less than 1% of the maximum efficiency.

The removal of metals reaches equilibrium within 5-10 minutes of contact time with best adjustments for pseudosecond order. The adsorption of metals by cassava adsorbents is better adjusted to the Freundlich model, with significant and critical information provided by Sips, Redlich-Peterson, Temkin, Liu, and Khan models.

Adsorption/desorption studies indicate that cassava adsorbents perform, on average, -10% of the adsorption of metals compared to activated carbon. Nevertheless, factors such as low cost and availability favor the use of such natural materials.

Data Availability

All figures, tables, photos, excel files, etc. will be provided to readers upon request.

Conflicts of Interest

The authors declare that they have no conflicts of interest.

Acknowledgments

This study was financed in part by the Coordenação de Aperfeiçoamento de Pessoal de Nível Superior–Brasil (CAPES)–Finance Code 001 and to the CNPq, for the research productivity scholarship (authors 2, 4, and 5). We are also grateful to the Department of Chemistry of the State University of Londrina (UEL, Brazil) for the assistance in carrying out the characterization evaluations (SEM and FTIR).

Supplementary Materials

Figure S1: pH_{PZC} obtained with KCl 0.5 M for CASS-BK (6.07), CASS-BA (6.23), and CASS-BB (6.37) and with KCl 0.05 M for CASS-BK (5.98), CASS-BA (5.85), and CASS-BB (6.15). Inside the graph, we highlighted the obtained average values for pH_{PCZ}. Figure S2: theoretical speciation of Cd^{2+}, Pb^{2+}, and Cr^{total}. Source: Software Hydromedusa, (Puigdomenech, 2018). Evaluated conditions: pH varying from 1.0 to 14.0; (ions) = 0.1 M. Figure S3: averages obtained for the study on cassava adsorbents (CASS-BK, CASS-BA, and BASS-BB) and their interaction with the pH of the solution (of Cd^{2+}, Pb^{+2}, and Cr^{total}) and the adsorbent doses. Experimental conditions: adsorbent doses tested from 4.0 to $24\ g\,L^{-1}$, pH evaluated from 4.0 to 7.0, stirring at 160 rpm, at 298 K for 1.5 h. Figure S4: adsorption isotherms for Cd^{2+} (from a to d), Pb^{2+} (from e to g), and Cr^{total} (from h to k) removal using cassava-based adsorbents CASS-BK, CASS-BA, and CASS-BB. Experimental conditions:

adsorbent dose of 8.0 g L^{-1}, pH of 5.5, stirring at 160 rpm for 60 min, at 298 K, heavy metal concentration varying from 5 to 200 mg L^{-1}. Table S1: some of the mathematical models (equations or expressions) used in this research. Table S2: summary of the infrared spectroscopy absorption by frequency regions (Figure 2) from before and after the adsorption of Cd^{2+}, Pb^{2+}, and Cr^{total}. Table S3: equations regarding the influence of pH and the adsorbent doses on removing Cd^{2+}, Pb^{2+}, and Cr^{total} by CASS-BK, CASS-BA, and CASS-BB and the graphical interpretation of Figure 3. Table S4: analysis of variance (ANOVA) for the removal of Cd, Pb, and Cr, for the causes of variation "Adsorbent" (CASS-BK, CASS-BA, and CASS-BB), "Adsorbent Doses" (4.0 to 24.0 g L^{-1}), and the "pH of the solution" (from 4.0 to 7.0). Table S5: Tukey's range test (at 5% of significance) for the removal of Cd^{2+}, Pb^{2+}, and Cr^{total}, in the evaluated pH ranges (4.0 to 7.0) and cassava adsorbents (CASS-BK, CASS-BA, and CASS-BB). Table S6: regression analysis coefficients for removing Cd^{2+}, Pb^{2+}, and Cr^{total} by the cassava biosorbents. Table S7: Tukey's range test for the interaction between the causes of variation "Adsorbent" (CASS-BK, CASS-BA, and CASS-BB) within every pH value (4.0, 5.0, 6.0, and 7.0) for the removal of Cd^{2+}, Pb^{2+}, and Cr^{total}. Table S8:ANOVA results on the goodness of the fit for the constructed isotherms. Table S9: Tukey's range test (at 5% significance) on the goodness of the fit for Cd^{2+}, Pb^{2+}, and Cr^{total} adsorption isotherms. References [62–72] describe further details in the supplementary material section. *(Supplementary Materials)*

References

[1] C. Bassegio, M. A. Campagnolo, D. Schwantes et al., "Growth and accumulation of Pb by roots and shoots of Brassica juncea L," *International Journal of Phytoremediation*, vol. 22, no. 2, pp. 134–139, 2019.

[2] WHO: World Health Organization, "Drinking-water: key facts," 2019, 2021, https://www.who.int/news-room/fact-sheets/detail/drinking-water.

[3] E. Conradi Jr., A. C. Gonçalves Jr., D. Schwantes et al., "Development of renewable adsorbent from cigarettes for lead removal from water," *Journal of Environmental Chemical Engineering*, vol. 7, no. 4, p. 103200, 2019.

[4] WHO: World Health Organization, *Guidelines for Drinking-water Quality*, 4th edition4th edition, , 2017.

[5] T. C. Alves, A. Pinheiro, D. Schwantes, and A. C. Gonçalves Jr., "Organic micropollutant adsorption in chemically modified forestry Pinus elliotti spp barks," *Journal of Solid Waste Technology and Management*, vol. 44, no. 2, pp. 142–152, 2018.

[6] M. Hassan, R. Naidu, J. Du, Y. Liu, and F. Qi, "Critical review of magnetic biosorbents: their preparation, application, and regeneration for wastewater treatment," *Science of the Total Environment*, vol. 702, p. 134893, 2020.

[7] D. Mehta, S. Mazumdar, and S. K. Singh, "Magnetic adsorbents for the treatment of water/wastewater–a review," *Journal of Water Process Engineering*, vol. 7, pp. 244–265, 2015.

[8] X. Xie, L. Zhang, X. Luo et al., "PEI modified magnetic porous cassava residue microspheres for adsorbing Cd(II) from aqueous solution," *European Polymer Journal*, vol. 159, p. 110741, 2021.

[9] EPA: Environmental Protection Agency, "Edition of the drinking water standards and health advisories tables (2018)," 2018, 2020, https://www.epa.gov/sites/production/files/2018-03/documents/dwtable2018.pdf.

[10] MINSAL, Ministerio de Salud: Decreto 131, "Reglamento de los servicios de agua destinados al consumo humano," 2007, 2020, http://bcn.cl/1y4j5.

[11] A. C. Gonçalves Jr., D. Schwantes, M. A. Campagnolo, D. C. Dragunski, and C. R. T. Tarley, "Removal of toxic metals using endocarp of açaí berry as biosorbent," *Water Science and Technology*, vol. 77, no. 6, pp. 1547–1557, 2018.

[12] D. Schwantes, A. C. Gonçalves Jr., A. de Varennes, and A. L. Braccini, "Modified grape stem as a renewable adsorbent for cadmium removal," *Water Science and Technology*, vol. 78, no. 11, pp. 2308–2320, 2018.

[13] D. Schwantes, A. C. Gonçalves Junior, G. F. Coelho et al., "Chemical modifications of cassava peel as adsorbent material for metals ions from wastewater," *Journal of Chemistry*, vol. 2016, 15 pages, 2016.

[14] R. Kayiwa, H. Kasedde, M. Lubwama, and J. B. Kirabia, "The potential for commercial scale production and application of activated carbon from cassava peels in Africa: a review," *Bioresource Technology Reports*, vol. 15, p. 100772, 2021.

[15] P. K. Sadh, S. Duhan, and J. S. Duhan, "Agro-industrial wastes and their utilization using solid state fermentation: a review," *Bioresources and Bioprocessing*, vol. 5, no. 1, p. 1, 2018.

[16] D. Schwantes, A. C. Gonçalves Jr., M. A. Campagnolo et al., "Chapter 15: use of co-products from the processing of cassava for the development of adsorbent materials aiming metal removal," in *Cassava (Intech Open)*, pp. 265–290, Viduranga Waisundara, 2017.

[17] A. O. Jorgetto, R. I. V. Silva, M. J. Saeki et al., "Cassava root husks powder as green adsorbent for the removal of Cu(II) from natural river water," *Applied Surface Science*, vol. 288, pp. 356–362, 2014.

[18] D. Schwantes, A. C. Gonçalves Jr., A. J. Miola, G. F. Coelho, M. G. Santos, and E. A. V. Leismann, "<b>Removal of Cu (II) and Zn (II) from water with natural adsorbents from cassava agroindustry residues," *Acta Scientiarum. Technology*, vol. 37, no. 3, pp. 409–417, 2015.

[19] Rajeshwarisivaraj, S. Sivakumar, P. Senthilkumar, and V. Subburam, "Carbon from cassava peel, an agricultural waste, as an adsorbent in the removal of dyes and metal ions from aqueous solution," *Bioresource Technology*, vol. 80, no. 3, pp. 233–235, 2001.

[20] C. O. Thompson, A. O. Ndukwe, and C. O. Asadu, "Application of activated biomass waste as an adsorbent for the removal of lead (II) ion from wastewater," *Emerging Contaminants.*, vol. 6, pp. 259–267, 2020.

[21] B. Welz and M. Sperling, *Atomic Absorption Spectrometry*, Wiley-VCH, Weinheim, 3rd edition, 2008.

[22] I. Puigdomenech, "Hydramedusa software," 2020, https://sites.google.com/site/chemdiagr/download?authuser=0.

[23] S. Lagergren, "Zur theorie der sogenannten adsorption geloster stoffe," *Kungliga Svenska Vetenskapsakademiens Handlingar.*, vol. 24, pp. 1–39, 1898.

[24] Y. S. Ho and G. Mckay, "A kinetic study of dye sorption by biosorbent waste product pith," *Resources, Conservation and Recycling*, vol. 25, no. 3-4, pp. 171–193, 1999.

[25] I. Langmuir, "The constitution and fundamental properties of solids and liquids. II. Liquids. 1," *Journal of the American Chemical Society*, vol. 39, no. 9, pp. 1848–1906, 1917.

[26] H. M. F. Freundlich, "Over the adsorption in solution," *The Journal of Physical Chemistry*, vol. 57, pp. 1100–1107, 1906.

[27] R. Sips, "On the structure of a catalyst surface," *The Journal of Chemical Physics*, vol. 16, no. 5, pp. 490–495, 1948.

[28] M. I. Temkin and V. Pyzhev, "Kinetics of ammonia synthesis on promoted iron catalysts," *Acta Physicochitnica UM.S.S*, vol. 12, pp. 327–356, 1940.

[29] O. Redlich and D. L. Peterson, "A useful adsorption isotherm," *The Journal of Physical Chemistry*, vol. 63, no. 6, p. 1024, 1959.

[30] J. Toth, "State equations of the solid gas interface layer," *Acta Chimica Hungarica*, vol. 69, pp. 311–317, 1971.

[31] Y. Liu, H. Xu, S.-F. Yang, and J.-H. Tay, "A general model for biosorption of Cd2+, Cu2+ and Zn2+ by aerobic granules," *Journal of Biotechnology*, vol. 102, pp. 233–239, 2013.

[32] A. R. Khan, I. R. Al-Waheab, and A. Al-Haddad, "A generalized equation for adsorption isotherms for multi-component organic pollutants in dilute aqueous solution," *Environmental Technology*, vol. 17, no. 1, pp. 13–23, 1996.

[33] A. R. Khan, R. Ataullah, and A. Al-Haddad, "Equilibrium adsorption studies of some aromatic pollutants from dilute aqueous solutions on activated carbon at different temperatures," *Journal of Colloid and Interface Science*, vol. 194, no. 1, pp. 154–165, 1997.

[34] D. F. Ferreira, "Sisvar: a computer analysis system to fixed effects split plot type designs," *Revista Brasileira de Biometria*, vol. 37, no. 4, pp. 529–535, 2019.

[35] H. Schulz and M. Baranska, "Identification and quantification of valuable plant substances by IR and Raman spectroscopy," *Vibrational Spectroscopy*, vol. 43, no. 1, pp. 13–25, 2007.

[36] D. Angin and S. Şensöz, "Effect of pyrolysis temperature on chemical and surface properties of biochar of rapeseed (Brassica napusL.)," *International Journal of Phytoremediation*, vol. 16, no. 7-8, pp. 684–693, 2014.

[37] LibreTexts, "Infrared spectroscopy absorption table," 2020, 2021, https://chem.libretexts.org/@go/page/22645.

[38] R. M. Silverstein, F. X. Webster, D. J. Kiemle, and D. L. Bryce, *Spectrometric Identification of Organic Compounds*, John Wiley & Sons, Inc., Hoboken, New Jersey, 8th edition, 2014.

[39] Brasil, *Resolution N° 357, 17th March 2005*, Brazilian National Council for the Environment, 2005, 2021, http://2.mma.gov.br/port/conama/legiabre.cfm?codlegi=459.

[40] A. C. Gonçalves Junior, A. L. Braccini, D. Schwantes et al., "Adsorbents developed from residual biomass of canola grains for the removal of lead from water," *Desalination and Water Treatment*, vol. 197, pp. 261–279, 2020.

[41] A. C. Gonçalves Junior, D. Schwantes, E. Conradi Junior, J. Zimmermann, and G. F. Coelho, "Adsorption of Cd (II), Pb (II) and Cr (III) on chemically modified Euterpe Oleracea," *Acta Scientiarum. Technology*, vol. 43, pp. 1–22, 2021.

[42] D. Schwantes, A. C. Gonçalves Jr., E. Conradi Junior, M. A. Campagnolo, and J. Zimmermann, "Determination of chlorpyrifos by GC/ECD in water and its sorption mechanism study in a Rhodic Ferralsol," *Journal of Environmental Health Science and Engineering*, vol. 18, no. 1, pp. 149–162, 2020.

[43] D. Schwantes, A. C. Gonçalves Jr., A. P. Schiller, J. Manfrin, L. A. V. Bianco, and A. G. Rosenberger, "Eco-friendly, renewable Crambe abyssinica Hochst-based adsorbents remove high quantities of Zn^{2+} in water," *Journal of Environmental Health Science and Engineering*, vol. 18, no. 2, pp. 809–823, 2020.

[44] J. J. Silveira Neta, C. J. Silva, G. C. Moreira, C. Reis, and E. L. Reis, "Remoção dos corantes Reactive Blue 21 e Direct Red 80 utilizando resíduos de sementes de Mabea fistulifera Mart. como biossorvente," *Ambiente & Água*, vol. 7, no. 1, pp. 104–119, 2012.

[45] J. Wu, J. Yang, G. Huang, C. Xu, and B. Lin, "Hydrothermal carbonization synthesis of cassava slag biochar with excellent adsorption performance for rhodamine B," *Journal of Cleaner Production*, vol. 251, p. 119717, 2020.

[46] M. Chen, X. Wang, and H. Zhang, "Comparative research on selective adsorption of Pb(II) by biosorbents prepared by two kinds of modifying waste biomass: highly-efficient performance, application and mechanism," *Journal of Environmental Management*, vol. 288, p. 112388, 2021.

[47] N. Ayawei, A. N. Ebelegi, and D. Wankasi, "Modelling and interpretation of adsorption isotherms," *Journal of Chemistry*, vol. 2017, Article ID 3039817, 11 pages, 2017.

[48] A. O. Data, A. P. Olalekan, A. M. Olatunya, and O. Dada, "Langmuir, Freundlich, Temkin and Dubinin-Radushkevich isotherms studies of equilibrium sorption of Zn2+ unto phosphoric acid modified rice husk," *Journal of Applied Chemistry*, vol. 3, no. 1, 45 pages, 2012.

[49] A. F. Taiwo and N. J. Chinyere, "Sorption Characteristics for Multiple Adsorption of Heavy Metal Ions Using Activated Carbon from Nigerian Bamboo," *Journal of Materials Science and Chemical Engineering*, vol. 4, no. 4, pp. 39–48, 2016.

[50] S. I. Mohammadabadi and V. Javanbakht, "Lignin extraction from barley straw using ultrasound-assisted treatment method for a lignin-based biocomposite preparation with remarkable adsorption capacity for heavy metal," *International Journal of Biology*, vol. 164, pp. 1133–1148, 2020.

[51] A. Nethaji, A. Sivasamy, and A. B. Mandal, "Adsorption isotherms, kinetics and mechanism for the adsorption of cationic and anionic dyes onto carbonaceous particles prepared from Juglans regia shell biomass," *International Journal of Environmental Science and Technology*, vol. 10, no. 2, pp. 231–242, 2013.

[52] M. A. Al-Ghouti and D. A. Da'ana, "Guidelines for the use and interpretation of adsorption isotherm models: a review," *Journal of Hazardous Materials*, vol. 393, p. 122383, 2020.

[53] N. M. Nimbalkar and R. B. Bhat, "Simultaneous adsorption of methylene blue and heavy metals from water using Zr-MOF having free carboxylic group," *Journal of Environmental Chemical Engineering*, vol. 9, no. 5, p. 106216, 2021.

[54] M. B. Ali, F. Wang, R. Boukherroub, and M. Xia, "High performance of phytic acid-functionalized spherical polyphenylglycine particles for removal of heavy metal ions," *Applied Surface Science*, vol. 518, p. 146206, 2020.

[55] M. F. Machado, C. P. Bergmann, E. C. Lima, M. A. Adebayo, and S. B. Fagan, "Adsorption of a textile dye from aqueous solutions by carbon nanotubes," *Materials Research*, vol. 17, Suppl. 1, pp. 153–160, 2014.

[56] R. Ramadoss and D. Subramaniam, "Removal of divalent nickel from aqueous solution using blue-green marine algae: adsorption modeling and applicability of various isotherm models," *Separation Science and Technology*, vol. 54, no. 6, pp. 943–961, 2018.

[57] C. Guo, L. Ding, X. Jin, H. Zhang, and D. Zhang, "Application of response surface methodology to optimize chromium (VI)

removal from aqueous solution by cassava sludge-based activated carbon," *Journal of Environmental Chemical Engineering*, vol. 9, no. 1, p. 104785, 2021.

[58] F. B. Scheufele, J. Staudt, M. H. Ueda et al., "Biosorption of direct black dye by cassava root husks: kinetics, equilibrium, thermodynamics and mechanism assessment," *Journal of Environmental Chemical Engineering*, vol. 8, no. 2, article 103533, 2020.

[59] J. Manfrin, A. C. Gonçalves Junior, D. Schwantes, E. Conardi Junior, J. Zimmermann, and G. L. Ziemer, "Development of biochar and activated carbon from cigarettes wastes and their applications in Pb^{2+} adsorption," *Journal of Environmental Chemical Engineering*, vol. 9, no. 2, p. 104980, 2021.

[60] N. Barka, M. Abdennouri, A. Boussaoud, and M. E. Makhfouk, "Biosorption characteristics of cadmium(II) onto _Scolymus hispanicus_ L. as low-cost natural biosorbent," *Desalination*, vol. 258, no. 1-3, pp. 66–71, 2010.

[61] P. K. Adapa, L. G. Tabil, G. J. Schoenau, T. Canam, and T. Dumonceaux, "Quantitative analysis of lignocellulosic components of non-treated and steam exploded barley, canola, oat and wheat straw using Fourier transform infrared spectroscopy," *Journal of Agricultural Science and Technology B*, vol. 1, pp. 177–188, 2011.

[62] ATSDR: Agency for Toxic Substances & Disease Registry, "Cadmium," 2020, 2020, http://www.atsdr.cdc.gov/substances/toxsubstance.asp?toxid=15.

[63] ATSDR: Agency for Toxic Substances & Disease Registry, "Lead," 2020, 2020, https://www.atsdr.cdc.gov/substances/toxsubstance.asp?toxid=22.

[64] ATSDR: Agency for Toxic Substances & Disease Registry, "Chromium," 2020, 2020, https://www.atsdr.cdc.gov/substances/toxsubstance.asp?toxid=17.

[65] ATSDR: Agency for Toxic Substances & Disease Registry, "ATSDR's ATSDR's substance priority list," 2019, 2020, https://www.atsdr.cdc.gov/spl/index.html.

[66] A. Bakshi and A. K. Panigrahi, "A comprehensive review on chromium induced alterations in fresh water fishes," *Toxicology Reports*, vol. 5, pp. 440–447, 2018.

[67] D. Đukić-Ćosić, K. Baralić, D. Javorac, A. B. Đorđević, and Z. Bulat, "An overview of molecular mechanisms in cadmium toxicity," *Current Opinion in Toxicology*, vol. 19, pp. 56–62, 2020.

[68] Y. Hamid, L. Tang, M. I. Sohail et al., "An explanation of soil amendments to reduce cadmium phytoavailability and transfer to food chain," *Science of the Total Environment*, vol. 660, pp. 80–96, 2019.

[69] A. Kubier, R. T. Wilkin, and T. Pichler, "Cadmium in soils and groundwater: a review," *Applied Geochemistry*, vol. 108, p. 104388, 2019.

[70] G. W. Latimer, *Official Methods of Analysis of AOAC International*, Association of Official Agricultural Chemists, Maryland, 20th edition, 2016.

[71] R. Levin, C. L. Z. Vieira, D. C. Mordarski, and M. H. Rosenbaum, "Lead seasonality in humans, animals, and the natural environment," *Environmental Research*, vol. 180, p. 108797, 2020.

[72] A. K. Tiwari, S. Orioli, and M. de Maio, "Assessment of groundwater geochemistry and diffusion of hexavalent chromium contamination in an industrial town of Italy," *Journal of Contaminant Hydrology*, vol. 225, p. 103503, 2019.